Table 1. Biological processes for genes up-regulated in HCC-infiltrating mononuclear inflammatory cells

Biological process	−log(*P*)	Gene	ID	*t* (*T/†NT)	*P*	Cellular components‡
Antigen presentation	8.526	CD163	NM_004244	3.96	0.001	M
		CD86 antigen	NM_006889	3.28	0.006	M
		IFN, α-inducible protein 6	NM_022872	2.99	0.031	M
		IFN, γ-inducible protein 30	NM_006332	2.89	0.011	M
		Fc fragment of IgG, high affinity Ia, receptor (CD64)	NM_000566	2.85	0.013	M
		C-type lectin domain family 4, member M	NM_014257	2.73	0.020	
		CD63	NM_001780	2.51	0.024	M
		CD1D antigen	NM_001766	2.19	0.049	
Ubiqutin-proteasomeal proteolysis	6.555	Nucleoporin 107 kDa	NM_020401	4.32	0.001	
		Proteasome subunit, β type, 5	NM_002797	3.80	0.002	T, M
		Ubiquitin-conjugating enzyme E2R 2	NM_017811	3.67	0.004	
		Proteasome subunit, α type, 5	NM_002790	3.64	0.003	
		Prostaglandin E synthase 3	NM_006601	3.53	0.003	
		Ubiquitin-conjugating enzyme E2 binding protein, 1	NM_005744	2.94	0.011	
		Ubiquitin-conjugating enzyme E2E 3	NM_006357	2.75	0.017	
		Dnaj (Hsp40) homologue, subfamily A, member 1	NM_001539	2.47	0.028	
		Syntaxin 5	BC012137	2.19	0.046	
ER and cytoplasm	5.704	Chaperonin containing TCP1, subunit 8 (θ)	NM_006585	3.71	0.002	T, M
		Peptidylprolyl isomerase A	NM_021130	3.69	0.002	
		ERO1-like	NM_014584	3.03	0.009	T, M
		Peptidylprolyl isomerase C	BC002678	2.68	0.017	M
		SEC63 homologue	AF119883	2.59	0.020	
		Peptidylprolyl isomerase B	NM_000942	2.54	0.023	
		Chaperonin containing TCP1, subunit 4 (δ)	NM_006430	2.53	0.023	
		FK506 binding protein 3, 25 kDa	NM_002013	2.46	0.026	T, M
		Heat shock 70 kDa protein 5	AF188611	2.45	0.027	
mRNA processing	5.143	Small nuclear ribonucleoprotein polypeptide B	NM_003092	4.65	0.000	
		Small nuclear ribonucleoprotein polypeptide F	BC002505	3.28	0.005	T
		DEAD (Asp-Glu-Ala-Asp) box polypeptide 20	NM_007204	3.22	0.006	
		Cleavage and polyadenylation specific factor 6	NM_007007	3.16	0.010	
		Cleavage stimulation factor subunit 2	NM_001325	3.10	0.008	T
		Heterogeneous nuclear ribonucleoprotein A2/B1	NM_031243	2.94	0.010	
		PRP4 pre-mRNA processing factor 4 homologue B	NM_003913	2.90	0.020	
		Gem-associated protein 4	NM_015721	2.64	0.019	T
		LSM6 homologue	NM_007080	2.63	0.019	
		Exportin 1	NM_003400	2.42	0.029	
		RNA-binding motif protein 8A	AF127761	2.41	0.030	
		Splicing factor, arginine/serine-rich 1	M72709	2.39	0.036	
Transcription by RNA polymerase II	4.298	TAF9 RNA polymerase II	NM_016283	5.01	0.001	
		General transcription factor IIH, polypeptide 3, 34 kDa	NM_001516	4.74	0.001	
		TAF6-like RNA polymerase II	NM_006473	3.91	0.002	
		Nuclear receptor corepressor 1	AF044209	3.64	0.007	
		TATA box binding protein	NM_003194	2.89	0.018	

(*Continued on the following page*)

Table 1. Biological processes for genes up-regulated in HCC-infiltrating mononuclear inflammatory cells (Cont'd)

Biological process	−log(*P*)	Gene	ID	*t* (*T/†NT)	*P*	Cellular components‡
		Cofactor required for Sp1 transcriptional activation	NM_004270	2.82	0.014	T, M
		SUB1 homologue	NM_006713	2.59	0.021	
		General transcription factor II, I	NM_033001	2.55	0.023	T, M
		GCN5-like 2	NM_021078	2.34	0.048	
		TBP-like 1	NM_004865	2.24	0.043	
Double-strand breaks repair	3.289	RAD51 homologue C	NM_058216	5.24	0.000	T
		Werner syndrome	AF091214	4.99	0.000	T
		NIMA-related kinase 1	AK027580	3.27	0.007	
		Protein phosphatase 2	AF086924	3.24	0.023	
		Protein phosphatase 6	NM_002721	3.13	0.007	
		Proliferating cell nuclear antigen	NM_002592	2.80	0.014	T
		Topoisomerase II α-4	AF285159	2.57	0.033	T
ESR1-nuclear pathway	2.886	Nuclear receptor corepressor 1	AF044209	3.64	0.007	
		Nuclear receptor coactivator 4	X77548	3.19	0.007	
		Dopachrome tautomerase	NM_001922	3.04	0.019	
		COP9, subunit 5	NM_006837	2.77	0.014	
		Tissue specific extinguisher 1	NM_002734	2.70	0.018	M
		SCAN domain containing 1	NM_033630	2.50	0.026	
		Kinase insert domain receptor	NM_002253	2.35	0.047	
Cell cycle	2.241	Cyclin-dependent kinase inhibitor 3	NM_005192	4.60	0.000	
		Erythrocyte membrane protein band 4.1	NM_004437	3.47	0.014	
		RAN, member RAS oncogene family	NM_006325	3.38	0.004	T
		Cyclin C	NM_005190	3.14	0.008	
		Cell division cycle 42	NM_044472	3.14	0.007	
		Cyclin-dependent kinase-like 1	NM_004196	2.77	0.033	
		Cell division cycle 73	NM_024529	2.72	0.043	M
		Cell division cycle 27	NM_001256	2.57	0.043	
		Microtubule-actin cross-linking factor 1	AK023285	2.57	0.025	
		Histone cluster 1	NM_005323	2.30	0.047	
		Cyclin-dependent kinase 7	NM_001799	2.13	0.050	
		Cyclin G_2	NM_004354	2.48	0.038	
Response to hypoxia and oxidative stress	1.401	Thioredoxin	NM_003329	2.64	0.019	T, M
		Glutaredoxin 2	NM_016066	2.63	0.024	T, M
		Peroxiredoxin 3	NM_006793	2.81	0.016	T, M
		Peroxiredoxin 2	NM_005809	2.27	0.039	
		Antioxidant protein 2	NM_004905	2.22	0.042	
		Peroxiredoxin 1	NM_002574	2.21	0.043	T, M
		Microsomal glutathione *S*-transferase 2	NM_002413	2.41	0.031	M

*T represents tumor-infiltrating mononuclear inflammatory cells.
†NT represents non-tumor-infiltrating mononuclear inflammatory cells.
‡Cellular components predominantly expressed cellular components among 26 immune regulatory cells (T, Th cells; M, macrophage).

unchanged genes in all samples (genes with less than a 1.8-fold difference in >85% of samples) to remove noise. This hierarchical clustering analysis using 1,917 filtered genes confirmed two clear clusters in patients with or without HCC (Fig. 2*A*). In one major cluster, including the most LC cases, there was a subcluster, LC/HCC, which included more of the HCC patients located next to the cluster of patients with HCC (LC/HCC; Fig. 2*A*). The reproducibility of the clustering (proportion, averaged over replications and over all pairs of samples in the same cluster, BRB-ArrayTools) was 93%. Sensitivity and specificity to HCC in this cluster analysis is 88% and 76%, respectively. These cirrhotic patients without HCC were followed for at least a further 12 months to detect HCC; none of those in the LC group developed HCC over this time. The principal component analysis was performed with the filtered 1,917 genes and the two major groups; classifying LC and HCC were similarly observed (Fig. 2*B*).

To further confirm that gene expression in the PBMCs of patients with HCC was distinct from that in patients without HCC, analysis of PBMC gene expression was performed by a

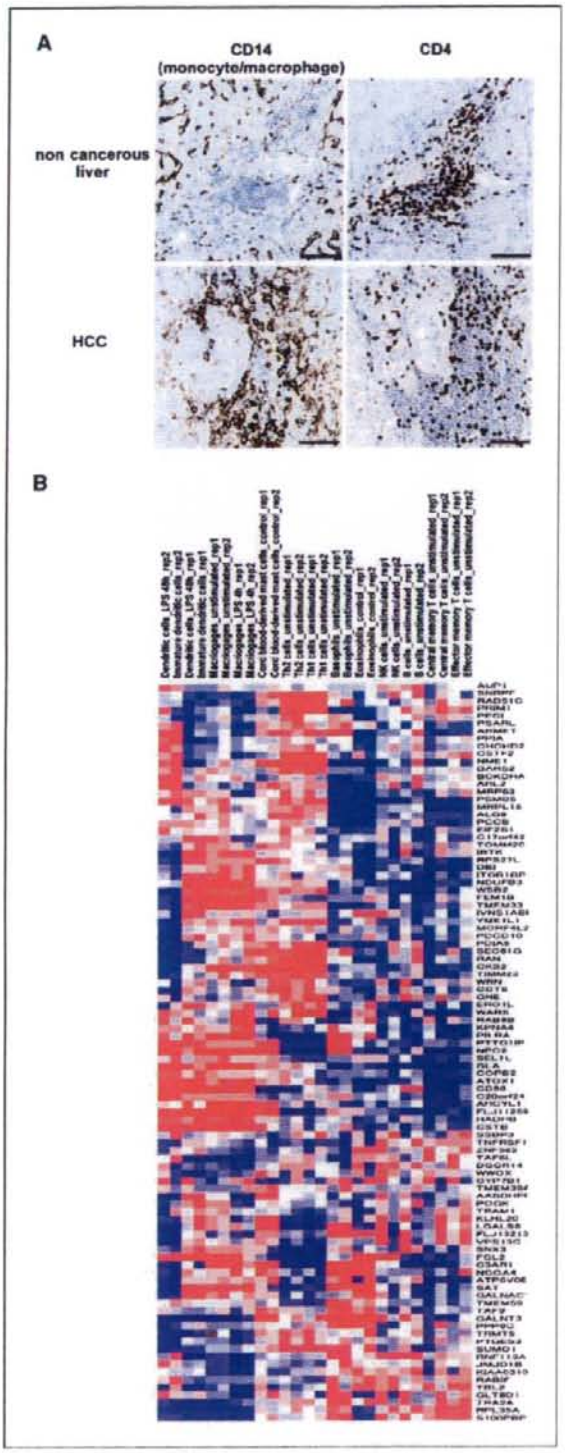

supervised learning method using categories of LC-C or HCC, age, gender, serum alanine aminotransferase (ALT), and α-fetoprotein (AFP). It showed that patients with or without HCC were significant classifiers ($P < 0.0005$), assigned with 1,430 predictor genes ($P < 0.002$; Table 2). Of 32 patients with LC, eight (25%) were misclassified as having HCC, and 2 of 30 patients with HCC (6.7%) were misclassified as not having HCC, indicating that the overall accuracy of the prediction of a patient with or without HCC was 84% (Table 2). Other clinical variables supposed to be related to HCC occurrence, such as age (ref. 29; >68 or ≤ 68 years old), gender (30), and ALT(ref. 31; >50 or ≤50 IU/L), could not differentiate gene expression in PBMCs. AFP (>20 or ≤20 ng/mL) was actually significant but was a much less powerful classifier ($P < 0.02$, assigned with 301 classifier genes). The prediction accuracy for categories of LC-C versus HCC and the AFP value >20 versus ≤20 ng/mL is not significantly affected whenever the number of predictor genes is reduced to below 62 (Supplementary Fig. S2). Taken together, these results by unsupervised and supervised analysis methods indicate that HCC development in LC-C patients significantly affects the gene expression profile in PBMCs.

Features of biological processes for which gene expression was significantly altered in PBMCs in HCC patients. We next examined the biological processes possibly affected by HCC development, given the expression profiles in PBMCs from patients with HCC. Statistical analysis showed that 867 genes were up-regulated and 989 genes were down-regulated in PBMCs from patients with HCC, compared with those without HCC ($P < 0.005$). Six representative genes, *Ccr1, Hat, Map2k1ip1, PigB, Tlr2,* and *Sod2*, were randomly selected from genes which were biologically important and differentially expressed between LC and HCC groups, and their expression was confirmed by RTD-PCR (Supplementary Fig. S3*A*). To exclude the possibility of circulating cancer cells, we have also examined the expression of *Afp, Krt8, Krt18,* and *Krt19*. No expression was detected for *Afp* (data not shown), and no statistically significant difference was found for expression of *Krt8, Krt18,* and *Krt19* between patients with HCC and without HCC (Supplementary Fig. S3*A*). The expression data were also confirmed by flow cytometric analysis. We evaluated how many cells in blood expressed CCR1 and CCR2 and confirmed that populations expressing CCR1 and CCR2 were significantly higher in PBMCs from patients with HCC than those without (Supplementary Fig. S3*B*). To understand the biological processes in PBMCs for which up-regulated or

Figure 1. HCC-infiltrating mononuclear inflammatory cells involve monocyte/macrophage and helper T cell. *A*, immunohistochemical staining. Many of the HCC-infiltrating mononuclear inflammatory cells expressed monocyte/macrophage marker, CD14. In contrast, few CD14-positive cells were seen in noncancerous liver-infiltrating mononuclear inflammatory cells. *Bars*, 100 μm. *B*, one-way hierarchical clustering analysis of gene expression of immune-mediating cells with genes whose expression was up-regulated in HCC-infiltrating mononuclear inflammatory cells. Data for gene expression in immune-mediating cells were retrieved from Gene Expression Omnibus[2] (Geo accession no. GDS 1775). By excluding genes missing from over half of the immune-mediating cells, 206 genes up-regulated in HCC-infiltrating mononuclear inflammatory cells were filtered, and the remaining 97 genes were used for clustering. Transverse and longitudinal titles show the type of immune-mediating cell and gene symbols, respectively. Color indicates relative expression magnitude of 97 up-regulated genes HCC-infiltrating mononuclear inflammatory cells among retrieved expression data of major leukocyte types deposited in the public database. The red and blue color means relatively high or low magnitude of expression among 26 retrieved expression data of leukocytes. The heat-map shows that helper T cells and unstimulated or stimulated macrophages included more blocks with the red color.

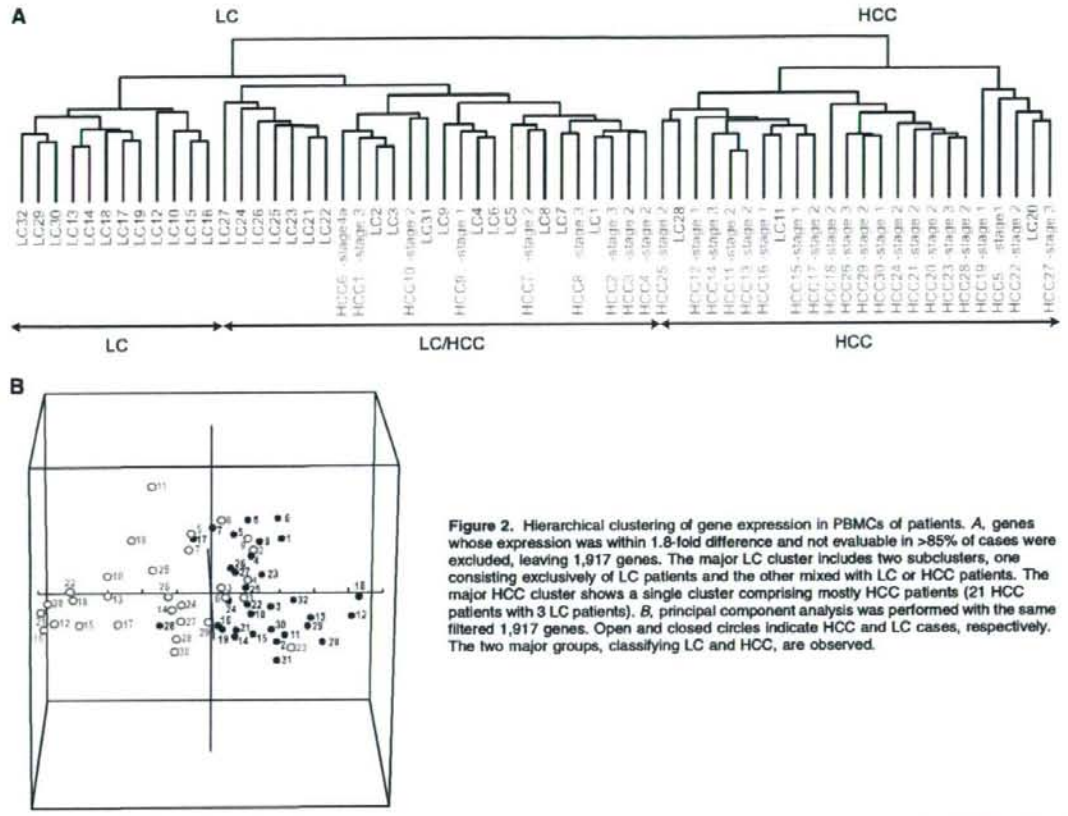

Figure 2. Hierarchical clustering of gene expression in PBMCs of patients. *A*, genes whose expression was within 1.8-fold difference and not evaluable in >85% of cases were excluded, leaving 1,917 genes. The major LC cluster includes two subclusters, one consisting exclusively of LC patients and the other mixed with LC or HCC patients. The major HCC cluster shows a single cluster comprising mostly HCC patients (21 HCC patients with 3 LC patients). *B*, principal component analysis was performed with the same filtered 1,917 genes. Open and closed circles indicate HCC and LC cases, respectively. The two major groups, classifying LC and HCC, are observed.

down-regulated genes were observed, we used MetaCore. The up-regulated genes in PBMCs from patients with HCC were involved in processes such as ubiquitin-proteasomal proteolysis (e.g., heat shock 70 kDa protein 4, ubiquitin conjugating enzymes), mRNA processing (e.g., heterogeneous nuclear ribonucleoproteins, RNA methyltransferase), antigen presentation (e.g., MHC class I polypeptide-related sequence A, B), cell cycle (e.g., HAT1, PCNA), and the response to hypoxia and oxidative stress (e.g., glutaredoxin 2, SOD2, thioredoxin; Table 3). These differentially up-regulated biological processes were also up-regulated processes in HCC-infiltrating inflammatory cells (Table 1). Thus, PBMCs from HCC patients present antigens in conditions of hypoxia and oxidative stress. Additionally, genes involved in other processes, such as apoptosis (e.g., apoptotic peptidase activating factor 1,

Table 2. Supervised learning methods for gene expression of PBMCs

Classifier category	Clinical groups	Total no. cases	No. cases misclassified	Classifier *P* values	No. genes in the classifiers ($P < 0.002$)
LC-C versus HCC	LC-C	32	8	<0.0005	1,430
	HCC	30	2		
Age (y)	>68	31	12	0.317	32
	≦68	31	16		
Gender	Male	25	15	0.178	20
	Female	37	9		
ALT (IU/L)	>50	26	20	0.82	28
	≦50	36	14		
AFP (ng/mL)	>20	29	10	0.02	301
	≦20	33	10		

Table 3. Biological processes for genes up-regulated in PBMCs of HCC patients

Biological process	−log(*P*)	Gene	ID	*t* (T/NT)	*P*	Cellular components
Ubiquitin-proteasomal proteolysis and ER	22.237	Ubiquitin specific peptidase 8	D29956	5.54	0.0000	
		Protein phosphatase 3 (formerly 2B),	NM_000945	4.90	0.0000	
		Heat shock transcription factor 2	NM_004506	4.52	0.0000	
		Heat shock 90 kDa protein 1	NM_005348	4.45	0.0000	T, M
		Ubiquitin protein ligase E3A	NM_000462	4.27	0.0001	
		Ubiquitin-conjugating enzyme E2D1	NM_003338	3.62	0.0006	M
		Phosphatidylinositol glycan, class B	NM_004855	3.57	0.0007	
		Ubiquitin-conjugating enzyme E2D2	NM_003339	3.49	0.0009	
		Ubiquitin-conjugating enzyme E2D3	NM_003340	3.18	0.0023	
		RAN binding protein 2	NM_006267	3.11	0.0029	
		Ubiquitin-conjugating enzyme E2A	NM_003336	3.09	0.0030	
		Activating transcription factor 6	NM_007348	3.03	0.0037	T, M
		Ubiquitin specific protease 7	NM_003470	2.92	0.0050	
		Heat shock 70 kDa protein 9B	NM_001746	2.91	0.0050	
		T-complex 1	NM_030752	2.76	0.0077	
		Glutaredoxin 2	NM_016066	2.70	0.0093	
		Ubiquitin-conjugating enzyme E2N	NM_003348	2.68	0.0096	
		Ubiquitin-conjugating enzyme E2 variant 2	AF049140	2.66	0.0110	
		Ubiquitin specific protease 14	NM_005151	2.20	0.0322	
		Progesterone receptor-associated p48 protein	NM_003932	2.16	0.0353	
		Heat shock 70 kDa protein 4	AB023420	2.16	0.0346	
		Ubiquitin-conjugating enzyme E2L 3	NM_003347	2.14	0.0363	
		Tenascin XB	NM_004381	2.13	0.0377	
		Ubiquitin specific peptidase 33	AB029020	2.12	0.0385	M
mRNA processing	20.087	Heterogeneous nuclear ribonucleoprotein R	NM_005826	3.90	0.0003	T
		RNA (guanine-7-) methyltransferase	NM_003799	3.29	0.0024	
		Heterogeneous nuclear ribonucleoprotein D-like	NM_031372	3.23	0.0020	
		Survival motor neuron domain containing 1	NM_005871	3.12	0.0031	
		Ribonueclease, rnase a family, 4	NM_002937	2.93	0.0052	
		Heterogeneous nuclear ribonucleoprotein A1	NM_002136	2.68	0.0094	
		Heterogeneous nuclear ribonucleoprotein K	NM_002140	2.46	0.0170	
		Heterogeneous nuclear ribonucleoprotein U	NM_031844	2.36	0.0216	
		UPF3, yeast, homologue of, A	NM_023011	2.35	0.0228	
		Alternative splicing factor	M72709	2.03	0.0471	
Antigen presentation	10.124	Janus kinase 1	NM_002227	3.38	0.0013	
		MHC, class II, DO α	NM_002119	3.09	0.0031	
		MHC, class II, DR α	NM_019111	2.67	0.0098	
		MHC class I polypeptide-related sequence B	NM_005931	2.60	0.0122	
		MHC class I polypeptide-related sequence A	NM_000247	2.26	0.0276	
		Tumor necrosis factor receptor–associated factor 6	NM_004620	2.05	0.0456	
Cell Cycle	6.185	Karyopherin (importin) β 2	NM_002270	4.32	0.0001	
		Histone acetyltransferase 1	NM_003642	4.15	0.0001	T, M
		V-myc myelocytomatosis viral oncogene homologue	NM_002467	3.57	0.0008	
		Transforming, acidic coiled-coil containing protein 1	NM_006283	3.38	0.0014	

(*Continued on the following page*)

Table 3. Biological processes for genes up-regulated in PBMCs of HCC patients (Cont'd)

Biological process	−log(*P*)	Gene	ID	*t* (T/NT)	*P*	Cellular components
		Centromere protein B, 80 kDa	X05299	3.37	0.0014	
		Conductin	AF078165	3.07	0.0032	
		Amyloid β precursor protein-binding protein 1	NM_003905	2.99	0.0040	T
		Centromere protein C 1	NM_001812	2.90	0.0054	
		Heterochromatin-like protein 1	BC000954	2.72	0.0085	
		Mature T-cell proliferation 1	BC002600	2.49	0.0154	
		Proliferating cell nuclear antigen	NM_002592	2.46	0.0166	
		CSE1 chromosome segregation 1-like	NM_001316	2.42	0.0186	M
		Karyopherin α4 (importin α3)	NM_002268	2.37	0.0209	
		Signal transducers and activators of transcription-like protein	BC010854	2.36	0.0214	
		M-phase phosphoprotein 6	NM_005792	2.34	0.0228	
		Extra spindle pole bodies homologue 1	NM_012291	2.20	0.0316	
Apoptosis	4.811	Cathepsin S	NM_004079	5.59	0.0000	M
		YME1-like 1	NM_014263	5.49	0.0000	T, M
		Cullin 5	NM_003478	4.65	0.0000	M
		Apoptotic peptidase activating factor 1	NM_001160	3.53	0.0008	
		Cullin 2	NM_003591	3.43	0.0012	M
		Amyloid β precursor protein-binding protein 1	NM_003905	2.99	0.0040	T
		Caspase 9	NM_032996	2.96	0.0044	
		F-box only protein 5	NM_012177	2.88	0.0055	
		Cullin 1	NM_003592	2.52	0.0146	
		Caspase 4	NM_001225	2.23	0.0293	
		Caspase 1	NM_033293	2.02	0.0475	
TCR signaling and immune related	5.462	Protein tyrosine phosphatase, receptor type, C	NM_002838	5.72	0.0000	
		Phosphoinositide-3-kinase, catalytic, α polypeptide	NM_006218	5.38	0.0000	
		Activating transcription factor 2	NM_001880	3.98	0.0002	
		Chemokine (c-c motif) receptor 1	NM_001295	3.90	0.0003	
		NCK adaptor protein 1	NM_006153	3.18	0.0024	
		Chemokine (c-c motif) receptor 2	NM_000647	2.78	0.0075	
		Toll-like receptor2	NM_003264	2.75	0.0078	
		Inositol 1,4,5-triphosphate receptor, type 1	NM_002222	2.24	0.0290	
		T-cell receptor α-chain	X01403	2.05	0.0452	
Response to hypoxia and oxidative stress	2.655	MAP2K1IP1	NM_021970	6.51	0.0000	
		Glutathione s-transferase θ 2	NM_000854	3.43	0.0011	
		Hypoxia-inducible factor 1, α subunit	NM_001530	2.99	0.0040	
		MAP/ERK kinase kinase 5	NM_005923	2.73	0.0086	
		Glutaredoxin 2	NM_016066	2.70	0.0093	
		Peroxiredoxin 3	NM_006793	2.68	0.0157	
		Catalase	NM_001752	2.50	0.0151	
		Plasma glutathione peroxidase 3 precursor	NM_002084	2.19	0.0329	
		Superoxide dismutase 2	NM_000636	2.10	0.0400	
		Thioredoxin	NM_003329	2.05	0.0186	

caspase 9) and T-cell receptor (TCR) signaling (e.g., CCR1, CCR2, TCR α-chain), were also up-regulated in PBMCs from patients with HCC, suggesting vulnerabilities of PBMCs and activated T-cell signaling, respectively, in HCC development.

Biological processes involving the down-regulated genes in PBMCs from patients with HCC included skeletal muscle development, the estrogen receptor 1 (ESR1) nuclear pathway, NOTCH signaling, feeding, and neurohormones signaling, neurogenesis, leptin signaling, and IL-12, IL-15, and IL-18 signaling (Supplementary Table S4), showing no obvious connection compared with the down-regulated genes in HCC-infiltrating mononuclear inflammatory cells (Supplementary Table S3). These results indicate that HCC development in cirrhotic liver can influence PBMCs, providing distinct transcriptional features of up-regulated genes even during the operable stage of HCCs.

Networks of genes commonly up-regulated or down-regulated in both PBMCs and HCC-infiltrating mononuclear inflammatory cells. Analysis of the gene expression profiles of HCC-infiltrating mononuclear inflammatory cells and PBMCs from HCC patients showed that the development of HCC altered the gene expression of local infiltrating mononuclear inflammatory cells and systemically circulating PBMCs; interestingly, the affected biological processes were largely the same. To further explore these presumed local and systemic influences resulting from HCC development, we examined how individual genes were affected by constructing a network.

We found 773 up-regulated and 750 down-regulated significant genes in HCC-infiltrating mononuclear inflammatory cells compared with noncancerous liver-infiltrating mononuclear inflammatory cells at the $P < 0.05$ level. In PBMC gene expression, we observed 2,111 up-regulated and 2,027 down-regulated genes in the PBMCs of HCC patients, compared with LC patients at the $P < 0.05$ level. Among these genes, 378 were significant in both HCC-infiltrating mononuclear inflammatory cells and PBMCs from patients with HCC (Fig. 3*A*). For these 378 genes commonly altered genes, 70% of them were up-regulated or down-regulated in both HCC-infiltrating mononuclear inflammatory cells and PBMCs from HCC patients, whereas expression of the remaining 30% of them was discordant.

We used MetaCore software to perform network construction for 172 up-regulated and 93 down-regulated genes in both HCC-infiltrating mononuclear inflammatory cells and PBMCs from HCC patients. The signal pathway network revealed three central genes, PCNA (32), SMAD3 (33), and nucleophosmin (34), which were all up-regulated in HCC-infiltrating mononuclear inflammatory cells and PBMCs from HCC patients (Fig. 3*B*). PCNA had interactions with proteasome subunit genes, PSMC2, PSMC6, PSMD12, and thioredoxin and DNA polymerase iota genes. SMAD3 was linked with cyclin-dependent kinase 7 and cyclin G_2 with various genes related to the cell cycle. Nucleophosmin was connected to ubiquitin-conjugating enzyme e2e3 and glutaredoxins. Notably, FOXP3, a marker of regulatory T cells, and Janus-activated kinase 3 (JAK3), related to interleukin signaling (35), were up-regulated and down-regulated, respectively, in HCC-infiltrating mononuclear inflammatory cells and PBMCs from HCC patients in the constructed gene network.

The network constructed for individual genes whose expression was commonly altered in HCC-infiltrating mononuclear inflammatory cells and PBMCs from HCC patients also supported a condition of HCC-related stress. The network also indicated that immune reactions in patients with HCC are complex, because down-regulated JAK3, an interleukin signaling molecule, and up-regulated FOXP3 and SMAD3, known molecules of anticancer immunity, are involved in this network. Biological processes in HCC-infiltrating mononuclear inflammatory cells and PBMCs from HCC patients also included the antigen-presentation process.

Discussion

In this study, we explored gene expression in local infiltrating mononuclear inflammatory cells in HCC and noncancerous liver tissues and in PBMCs obtained from patients with hepatitis C–related LC, with or without HCC. Gene expression profiles of HCC-infiltrating mononuclear inflammatory cells were quite distinct from those of noncancerous liver-infiltrating mononuclear inflammatory cells, showing their differing roles in anticancer immunity. We also investigated gene expression in systemically circulating PBMCs from LC-C patients with or without HCC and found that PBMC gene expression profiles from patients with or without HCC were significantly different. Intriguingly, many biological processes involving the up-regulated genes were shared between HCC-infiltrating mononuclear inflammatory cells and PBMCs from HCC patients, suggesting that the local inflammatory effect evoked by HCC development is systemically projected in the host.

Tumor-infiltrating mononuclear inflammatory cells have been investigated to examine their roles in local cancer tissues. We have selectively obtained aggregates of infiltrating mononuclear inflammatory cells in HCC and noncancerous liver tissues by LCM without contamination of carcinoma or parenchymal cells. We have shown that the process of antigen-presentation (36) is a distinguishing feature for up-regulated genes in HCC-infiltrating mononuclear inflammatory cells compared with noncancerous liver-infiltrating mononuclear inflammatory cells. Consistently, immunohistochemical staining of HCC and noncancerous liver tissues revealed that the HCC-infiltrating mononuclear inflammatory cells are primarily monocytes/macrophages, a lineage of phagocytes and antigen-presenting cells (37). Helper CD4 T cells were also found but seemed to be scattered in the HCC-infiltrating mononuclear inflammatory cells, compared with their intensive accumulation in infiltrating mononuclear inflammatory cells in noncancerous liver tissues. Correspondingly, analysis using a publicly available gene expression database of major leukocytes showed that up-regulated genes in HCC-infiltrating mononuclear inflammatory cells were primarily featured for macrophages and Th1 and Th2 CD4 cells, preconditioned with IL-12 and IL-4, respectively. These findings could be interpreted in that HCC expresses tumor-antigens (38) different from the surrounding noncancerous liver tissues; consequently, phagocytes gather in HCC tissues, take up antigens expressed by HCC tissues, and interact with CD4 cells (39). The scattered distribution and transcriptional features of both the Th1 and Th2 predisposed status of CD4 helper T cells in HCC-infiltrating mononuclear inflammatory cells suggests their versatile inflammatory status in cancer immunity, although there was no obvious shift of the Th1/Th2 balance, which is considered to be important in cancer immunity (40).

Other characteristic biological processes involving the up-regulated genes in HCC-infiltrating mononuclear inflammatory cells included the response to hypoxia and oxidative stress (41), the ubiquitin-proteasome system, cell cycle, mRNA processing, ER, and cytoplasm. The ubiquitin-proteasome system is unique to eukaryotic cells and important in maintaining the normal biological activity of cells, with pleiotropic effects in higher animals (42). The cell cycle requires precise regulation of cyclin-dependent kinase under strict control by ubiquitination and subsequent protein degradation (32). Taken together, these processes involving the up-regulated genes may reflect a protective local response of the host, corresponding to the stress environment of HCC. In this sense, the double-strand break repair gene up-regulation may be interpreted as the cells responding to maintain normal cellular activities although they are exposed to a harmful environment by the HCC (43).

The biological processes involving the up-regulated genes in PBMCs from HCC patients, compared with those from LC-C patients without HCC, were, to a substantial degree, the same, involving the up-regulated genes in HCC-infiltrating mononuclear

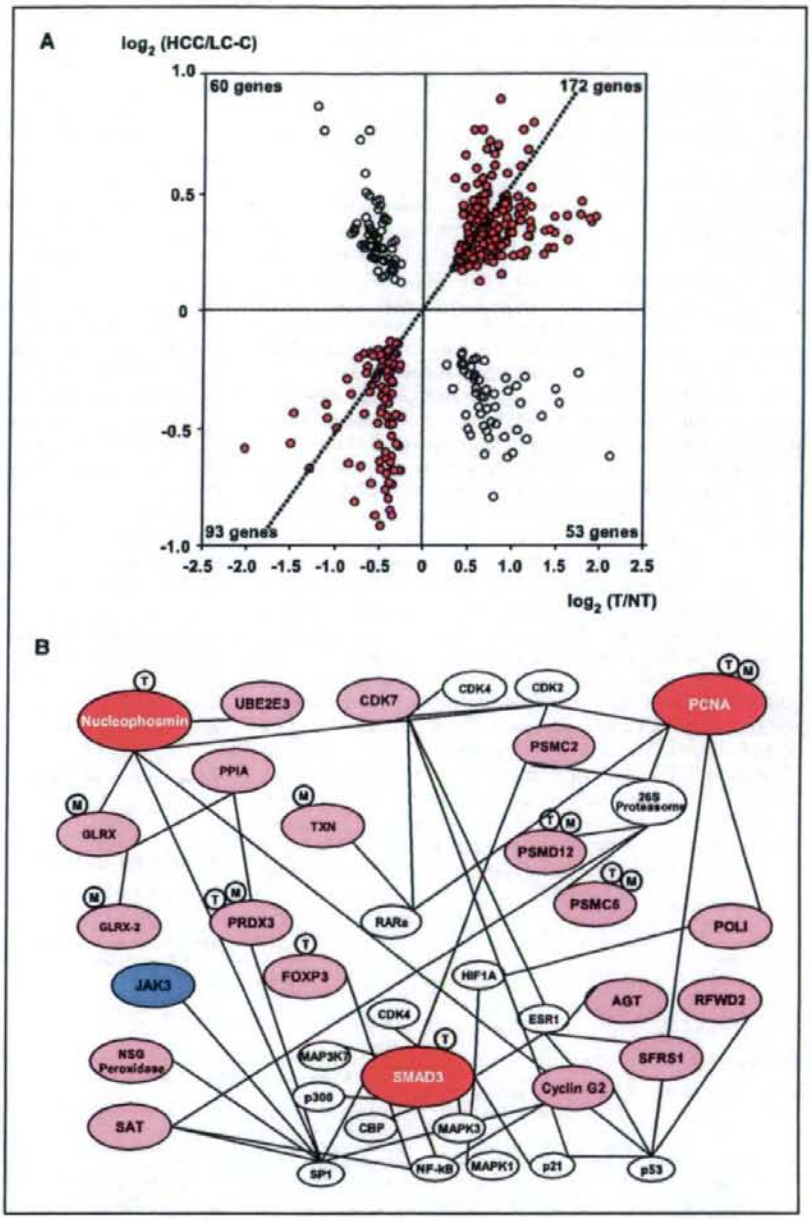

Figure 3. Features of commonly affected genes in PBMCs of HCC patients and HCC-infiltrating mononuclear inflammatory cells. *A*, scatter plots of gene expression ratios between local infiltrating mononuclear inflammatory cells and PBMCs. The axes show the binary logarithm value of the gene expression ratio of HCC-infiltrating mononuclear inflammatory cells over noncancerous liver-infiltrating mononuclear inflammatory cells on the *x* axis and the ratio of PBMCs from HCC patients over LC-C patients on the *y* axis. The right top quadrant includes 172 genes whose expression was up-regulated in HCC-infiltrating mononuclear inflammatory cells and in PBMCs from HCC patients, whereas the left bottom quadrant includes 93 genes down-regulated in both. *B*, interactive network for differentially expressed genes between PBMCs of HCC and LC-C patients and between infiltrating cells adjacent to HCC and noncancerous liver tissues. The three highlighted genes are PCNA, SMAD3, and nucleophosmin, which are related to the redox system, ubiquitin-proteasome system, and cell cycle, in addition to some immunologic gene connections. T or M at each node represent T lymphocytes or monocytes, respectively, and indicate the cell population in which each gene was expressed. The red-filled and blue-filled circles indicate up-regulation or down-regulation, respectively, in HCC-infiltrating mononuclear inflammatory cells and PBMCs from HCC patients.

inflammatory cells, such as ubiquitin-proteasomal proteolysis, ER, and cytoplasm, mRNA processing, antigen presentation, the cell cycle, and the response to hypoxia and oxidative stress. The reflection of these transcriptional features of HCC-infiltrating mononuclear inflammatory cells by PBMCs from HCC patients suggests a systemically projected influence of local HCC development, which is presumably the result of the stress environment caused by HCC and the host's reaction even when the size of the tumor is relatively small. In addition to exploring these biological processes, we also constructed networks of individual genes, the expression of which was similarly up-regulated or down-regulated, to depict commonly affected biological processes in tumor-infiltrating mononuclear inflammatory cells and PBMCs under HCC development in more detail. The networks highlighted three central genes, nucelophosmin, PCNA, and SMAD3, as up-regulated genes. They are connected to individual genes involved in ubiquitin,

proteasomes, the cell cycle, and oxidative stress (Fig. 3*B*). Interestingly, the immunologically important molecules, FOXP3 and JAK3, are in the network as up-regulated and down-regulated genes, respectively. FOXP3 is a transcriptional marker for regulatory T cells (44), and SMAD3 is also believed to be important in maintaining regulatory T cells (45). JAK3, which is associated with the interleukin receptor common γ chain (35) and is important in lymphoid development (46), was also involved in the network, suggesting that HCC influences the host immune system, which can be observed not only in HCC-infiltrating mononuclear inflammatory cells but also in the PBMCs of HCC patients. Thus, the network features of individual genes, commonly affected in HCC-infiltrating mononuclear inflammatory cells and PBMCs from HCC patients, further imply that the anticancer immunity of the host in response to HCC development involves the antigen presentation process to initiate the immune reaction.

The mechanism by which PBMCs from HCC patients reflect the transcriptional features of HCC-infiltrating mononuclear inflammatory cells requires further study. We observed that the population of CCR1-expressing and CCR2-expressing cells in PBMCs from HCC patients was higher than in those from LC-C patients. However, HCC-infiltrating mononuclear inflammatory cells did not show up-regulation of these genes. The meaning of the up-regulated CCR1 and CCR2 should be further investigated because chemokines are key molecules for the recruitment of inflammatory cells, regulating cellular adhesion and transendothelial migration, and the activation of inflammatory cells (47). The biological process of integrin-mediated cell matrix adhesion, genes involved in which were down-regulated in HCC-infiltrating mononuclear inflammatory cells, may suggest that these cells were able to remigrate into the microcirculation with the enriched blood flow in HCC tissues. The process of integrin-mediated cell matrix adhesion in HCC-infiltrating inflammatory cells may imply weaker adhesion of infiltrating mononuclear inflammatory cells to cancer tissues compared with noncancerous liver tissues (48). PBMCs are also presumed to be affected by humoral factors from HCC tissues (49). Another possibility is the presence of hematogenous spreading and circulating HCC cells because mRNA for AFP was detected in circulation (50). Because two-thirds of HCC patients enrolled for gene expression analysis of PBMCs showed serum AFP value <100, the presence of circulating HCC cells would not be evaluated by the detection of *Afp* gene expression alone. Therefore, we have examined expression of *Krt8, Krt18,* and *Krt19,* as well as *Afp*. Despite of the possibility of circulating cancer cells, we neither detected expression of *Afp* nor found significantly different expression of *Krt8, Krt18,* and *Krt19* between HCC and LC-C patients without HCC. Furthermore, genes up-regulated in HCC tissues compared with noncancerous liver tissues[3] did not correlate to up-regulated genes in PBMCs of HCC patients, indicating that different signature of gene expression in PBMCs between HCC and LC-C patients is not the reflection of the possible migrating cells from HCC tissues. In addition, all HCC cases, except for a case in gene expression analysis of PBMCs, were radiologically free of tumor thrombus in the vessel, which was indicative of microscopic invasion free or concomitant with invasion in the periphery of third or lower branch of vessels, suggesting that contribution of circulating cancer cells were presumed to be sufficiently small for the distinct difference of gene expression signature of PBMCs.

Although the number of enrolled HCC patients for analysis with local inflammatory cells was relatively small compared with the number of patients for analysis of PBMCs, our study has shown shared features of gene expression profiles of HCC-infiltrating mononuclear inflammatory cells and PBMCs from HCC patients, showing a complex immune status of the host in anticancer immunity. This finding suggests the possibility that readily accessible PBMCs can be used as a surrogate tissue to assess the local inflammatory environment surrounding cancers through examination of gene expression profiles.

Disclosure of Potential Conflicts of Interest

No potential conflicts of interest were disclosed.

Acknowledgments

Received 3/10/2008; revised 9/5/2008; accepted 9/25/2008.

The costs of publication of this article were defrayed in part by the payment of page charges. This article must therefore be hereby marked *advertisement* in accordance with 18 U.S.C. Section 1734 solely to indicate this fact.

We thank Nakamura for her invaluable contribution to this study.

[3] Unpublished data.

References

1. El-Serag HB, Mason AC. Rising incidence of hepatocellular carcinoma in the United States. N Engl J Med 1999;340:745–50.
2. Motola-Kuba D, Zamora-Valdes D, Uribe M, Mendez-Sanchez N. Hepatocellular carcinoma. An overview. Ann Hepatol 2006;5:16–24.
3. Yoshida H, Shiratori Y, Moriyama M, et al. Interferon therapy reduces the risk for hepatocellular carcinoma: national surveillance program of cirrhotic and noncirrhotic patients with chronic hepatitis C in Japan. IHIT Study Group. Inhibition of Hepatocarcinogenesis by Interferon Therapy. Ann Intern Med 1999;131:174–81.
4. Farinati F, Marino D, De Giorgio M, et al. Diagnostic and prognostic role of α-fetoprotein in hepatocellular carcinoma: both or neither? Am J Gastroenterol 2006; 101:524–32.
5. Yu P, Lee Y, Liu W, et al. Priming of naive T cells inside tumors leads to eradication of established tumors. Nat Immunol 2004;5:141–9.
6. Preynat-Seauve O, Schuler P, Contassot E, Beermann F, Huard B, French LE. Tumor-infiltrating dendritic cells are potent antigen-presenting cells able to activate T cells and mediate tumor rejection. J Immunol 2006;176: 61–7.
7. Kawata A, Une Y, Hosokawa M, Uchino J, Kobayashi H. Tumor-infiltrating lymphocytes and prognosis of hepatocellular carcinoma. Jpn J Clin Oncol 1992;22:256–63.
8. Hirano S, Iwashita Y, Sasaki A, Kai S, Ohta M, Kitano S. Increased mRNA expression of chemokines in hepatocellular carcinoma with tumor-infiltrating lymphocytes. J Gastroenterol Hepatol 2007;22:690–6.
9. Kobayashi N, Hiraoka N, Yamagami W, et al. FOXP3+ regulatory T cells affect the development and progression of hepatocarcinogenesis. Clin Cancer Res 2007;13: 902–11.
10. Williams MA, Newland AC, Kelsey SM. The potential for monocyte-mediated immunotherapy during infection and malignancy: Part I. Apoptosis induction and cytotoxic mechanisms. Leuk Lymphoma 1999;34:1–23.
11. Nakao M, Sata M, Saitsu H, et al. CD4+ hepatic cancer-specific cytotoxic T lymphocytes in patients with hepatocellular carcinoma. Cell Immunol 1997;177: 176–81.
12. Honda M, Kawai H, Shirota Y, Yamashita T, Kaneko S. Differential gene expression profiles in stage I primary biliary cirrhosis. Am J Gastroenterol 2005;100:2019–30.
13. Honda M, Yamashita T, Ueda T, Takatori H, Nishino R, Kaneko S. Different signaling pathways in the livers of patients with chronic hepatitis B or chronic hepatitis C. Hepatology 2006;44:1122–38.
14. Daiba A, Inaba N, Ando S, et al. A low-density cDNA microarray with a unique reference RNA: pattern recognition analysis for IFN efficacy prediction to HCV as a model. Biochem Biophys Res Commun 2004;315:1088–96.
15. Tateno M, Honda M, Kawamura T, Honda H, Kaneko S. Expression profiling of peripheral-blood mononuclear cells from patients with chronic hepatitis C undergoing interferon therapy. J Infect Dis 2007;195:255–67.
16. Takamura T, Honda M, Sakai Y, et al. Gene expression profiles in peripheral blood mononuclear cells reflect the pathophysiology of type 2 diabetes. Biochem Biophys Res Commun 2007;361:379–84.
17. Burczynski ME, Twine NC, Dukart G, et al. Transcriptional profiles in peripheral blood mononuclear cells prognostic of clinical outcomes in patients with advanced renal cell carcinoma. Clin Cancer Res 2005;11: 1181–9.

18. Matsui O. Imaging of multistep human hepatocarcinogenesis by CT during intra-arterial contrast injection. Intervirology 2004;47:271–6.
19. Sakai Y, Morrison BJ, Burke JD, et al. Vaccination by genetically modified dendritic cells expressing a truncated neu oncogene prevents development of breast cancer in transgenic mice. Cancer Res 2004;64:8022–8.
20. Wada Y, Nakashima O, Kutami R, Yamamoto O, Kojiro M. Clinicopathological study on hepatocellular carcinoma with lymphocytic infiltration. Hepatology 1998;27:407–14.
21. Fu J, Xu D, Liu Z, et al. Increased regulatory T cells correlate with CD8 T-cell impairment and poor survival in hepatocellular carcinoma patients. Gastroenterology 2007;132:2328–39.
22. Xu W, Roos A, Daha MR, van Kooten C. Dendritic cell and macrophage subsets in the handling of dying cells. Immunobiology 2006;211:567–75.
23. Gadola SD, Dulphy N, Salio M, Cerundolo V. Vα24-JαQ-independent, CD1d-restricted recognition of α-galactosylceramide by human CD4(+) and CD8αβ(+) T lymphocytes. J Immunol 2002;168:5514–20.
24. Feinberg H, Taylor ME, Weis WI. Scavenger receptor C-type lectin binds to the leukocyte cell surface glycan Lewis(x) by a novel mechanism. J Biol Chem 2007;282:17250–8.
25. Orabona C, Grohmann U, Belladonna ML, et al. CD28 induces immunostimulatory signals in dendritic cells via CD80 and CD86. Nat Immunol 2004;5:1134–42.
26. Demartino GN, Gillette TG. Proteasomes: machines for all reasons. Cell 2007;129:659–62.
27. Petruti-Mot AS, Earnshaw WC. Two differentially spliced forms of topoisomerase IIα and β mRNAs are conserved between birds and humans. Gene 2000;258:183–92.
28. Naryzhny SN, Desouza LV, Siu KW, Lee H. Characterization of the human proliferating cell nuclear antigen physico-chemical properties: aspects of double trimer stability. Biochem Cell Biol 2006;84:669–76.
29. Velazquez RF, Rodriguez M, Navascues CA, et al. Prospective analysis of risk factors for hepatocellular carcinoma in patients with liver cirrhosis. Hepatology 2003;37:520–7.
30. Ikeda K, Arase Y, Saitoh S, et al. Prediction model of hepatocarcinogenesis for patients with hepatitis C virus-related cirrhosis. Validation with internal and external cohorts. J Hepatol 2006;44:1089–97.
31. Tarao K, Rino Y, Ohkawa S, et al. Close association between high serum alanine aminotransferase levels and multicentric hepatocarcinogenesis in patients with hepatitis C virus-associated cirrhosis. Cancer 2002;94:1787–95.
32. Cayrol C, Ducommun B. Interaction with cyclin-dependent kinases and PCNA modulates proteasome-dependent degradation of p21. Oncogene 1998;17:2437–44.
33. Riggins GJ, Thiagalingam S, Rozenblum E, et al. Mad-related genes in the human. Nat Genet 1996;13:347–9.
34. Dhar SK, Lynn BC, Daosukho C, St Clair DK. Identification of nucleophosmin as an NF-κB co-activator for the induction of the human SOD2 gene. J Biol Chem 2004;279:28209–19.
35. Oakes SA, Candotti F, Johnston JA, et al. Signaling via IL-2 and IL-4 in JAK3-deficient severe combined immunodeficiency lymphocytes: JAK3-dependent and independent pathways. Immunity 1996;5:605–15.
36. Smyth MJ, Godfrey DI, Trapani JA. A fresh look at tumor immunosurveillance and immunotherapy. Nat Immunol 2001;2:293–9.
37. Dobrovolskaia MA, Vogel SN. Toll receptors, CD14, and macrophage activation and deactivation by LPS. Microbes Infect 2002;4:903–14.
38. Kim JW, Ye Q, Forgues M, et al. Cancer-associated molecular signature in the tissue samples of patients with cirrhosis. Hepatology 2004;39:518–27.
39. Itano AA, Jenkins MK. Antigen presentation to naive CD4 T cells in the lymph node. Nat Immunol 2003;4:733–9.
40. Budhu A, Wang XW. The role of cytokines in hepatocellular carcinoma. J Leukoc Biol 2006;80:1197–213.
41. Gerald D, Berra E, Frapart YM, et al. JunD reduces tumor angiogenesis by protecting cells from oxidative stress. Cell 2004;118:781–94.
42. Pickart CM. Back to the future with ubiquitin. Cell 2004;116:181–90.
43. Liu L, Simon MC. Regulation of transcription and translation by hypoxia. Cancer Biol Ther 2004;3:492–7.
44. Ramsdell F. Foxp3 and natural regulatory T cells: key to a cell lineage? Immunity 2003;19:165–8.
45. Fantini MC, Becker C, Monteleone G, Pallone F, Galle PR, Neurath MF. Cutting edge: TGF-β induces a regulatory phenotype in CD4+CD25- T cells through Foxp3 induction and down-regulation of Smad7. J Immunol 2004;172:5149–53.
46. Park SY, Saijo K, Takahashi T, et al. Developmental defects of lymphoid cells in Jak3 kinase-deficient mice. Immunity 1995;3:771–82.
47. Baggiolini M. Chemokines and leukocyte traffic. Nature 1998;392:565–8.
48. Leon MP, Bassendine MF, Gibbs P, Thick M, Kirby JA. Immunogenicity of biliary epithelium: study of the adhesive interaction with lymphocytes. Gastroenterology 1997;112:968–77.
49. Cao M, Cabrera R, Xu Y, et al. Hepatocellular carcinoma cell supernatants increase expansion and function of CD4(+)CD25(+) regulatory T cells. Lab Invest 2007;87:582–90.
50. Wong IH, Yeo W, Leung T, Lau WY, Johnson PJ. Circulating tumor cell mRNAs in peripheral blood from hepatocellular carcinoma patients under radiotherapy, surgical resection or chemotherapy: a quantitative evaluation. Cancer Lett 2001;167:183–91.

Optimal amount of monocyte chemoattractant protein-1 enhances antitumor effects of suicide gene therapy against hepatocellular carcinoma by M1 macrophage activation

Tomoya Tsuchiyama,[1] Yasunari Nakamoto,[1] Yoshio Sakai,[1] Naofumi Mukaida[2] and Shuichi Kaneko[1,3]

[1]Disease Control and Homeostasis, Graduate School of Medical Science, [2]Division of Molecular Bioregulation, Cancer Research Institute, Kanazawa University, 13-1 Takara-machi, Kanazawa 920-8641, Japan

(Received April 10, 2008/Revised June 18, 2008/Accepted June 27, 2008/Online publication October 9, 2008)

Suicide gene therapy combined with chemokines provides significant antitumor efficacy. Coexpression of suicide gene and monocyte chemoattractant protein-1 (MCP-1) increases antitumor effects in murine models of hepatocellular carcinoma (HCC) and colon cancer. However, it is unclear whether the doses administered achieved the maximum antitumor effects. We evaluated antitumor effects of various amounts of recombinant adenovirus vector (rAd) expressing MCP-1 in the presence of a suicide gene in a murine model of HCC. HCC cells were transplanted subcutaneously into BALB/c nude mice, and transduced with a fixed amount of Ad-tk harboring the suicide gene, *HSV-tk*, and various doses of Ad-MCP1 harboring MCP-1 (ratios of 1:1, 0.1:1, and 0.01:1 relative to Ad-tk). Growth of primary tumors was suppressed when treated with Ad-tk plus Ad-MCP1 (1:1 and 1:0.1) as compared with Ad-tk alone. The antitumor effects against tumor rechallenge tended to be high in the Ad-tk plus Ad-MCP1 group (1:0.1). The effects were dependent on production of Th1 type-cytokines. Delivery of an optimal amount of rAd expressing MCP-1 enhanced the antitumor effects of suicide gene therapy against HCC by M1 macrophage activation, suggesting that this is a plausible form of cancer gene therapy to prevent HCC progression and recurrence. (*Cancer Sci* 2008; 99: 2075–2082)

Cancer gene therapy using combinations of various genes, such as suicide and cytokine genes, to enhance tumor regression therapy is widely used.[1,2] Previously, we reported that the coexpression of herpes simplex virus thymidine kinase (HSV-tk) and monocyte chemoattractant protein-1 (MCP-1) showed enhanced antitumor effects in models of hepatocellular carcinoma (HCC)[3] and colon cancer,[4] and these antitumor effects were dependent on the activation of macrophages.[3] MCP-1 is a chemokine that regulates the recruitment of monocytes/macrophages to inflammatory sites and tumor tissues as well as their activation, including lysosomal enzyme release and tumoricidal activity,[5] and is functional in both mice and humans.[6] However, MCP-1 was reported to be destructive in some tumor models,[6,7] but protective in others.[8] Monocytes/macrophages recruited by MCP-1 have dual functions in that they can prevent the establishment and spread of tumor cells,[6] and simultaneously support tumor growth and dissemination.[8] This ambivalent relationship reflects the elevated functional plasticity of macrophages, which are able to express different functional programs in response to different microenvironment signals, as exemplified in the M1 (classical)–M2 (alternative or non-classical) paradigm of macrophage polarization.[9]

On the other hand, although double infection methods are used to enhance antitumor effects in cancer gene therapy, significant antitumor effects have been reported in some studies,[4,10] but not in others.[11,12] Moreover, it is not clear how the antitumor effects are affected by differences in the doses administered. In the present study, various amounts of recombinant adenovirus vector (rAd) expressing the *MCP-1* gene were delivered into cells along with the same amount of HSV-tk to determine the optimal dosage of MCP-1 for induction of stronger antitumor effects in double infection methods. Furthermore, we also examined the involvement of macrophage immune responses in these effects. Here, we demonstrated that treatment with the 1:0.1 ratio of Ad-HSV-tk (Ad-tk) plus Ad-MCP1 tended to exert antitumor immunity, suggesting that there may be an optimal amount of Ad-MCP1 in suicide gene therapy. In addition, it is possible that the antitumor responses seen in the HSV-tk plus MCP-1 system were associated with increased Th1 (T helper 1)–type cytokine production by activated M1 macrophage. These findings will be of value in cancer gene therapy.

Materials and Methods

Recombinant adenoviruses. rAds harboring the human MCP-1 (Ad-MCP1), HSV-tk (Ad-tk), and lacZ (Ad-lacZ), and driven by the CAG promoter were prepared, purified, and titrated according to the protocols supplied by the manufacturer (Takara Bio, Shiga, Japan), as described.[13] The rAds were purified on cesium gradients and their titers were determined by the 50% tissue culture infectious dose ($TCID_{50}$).

Cell lines and culture. The human HCC cell line Huh7 and the mouse HCC cell line BNL 1ME A.7R.1 (BNL) were cultured in Dulbecco's minimal essential medium (Gibco, Long Island, NY, USA) supplemented with 10% heat-inactivated fetal bovine serum (Gibco).

Enzyme-linked immunosorbent assay (ELISA) for MCP-1. Aliquots of 1×10^5 Huh7 cells were seeded in 1.0 mL of culture media in 24-well tissue culture plates. Twenty-four h later, the cells were infected with each rAd at a multiplicity of infection (MOI) of 10, and the medium was collected 48 h later. On the other hand, in some experiments, ganciclovir (GCV; Tanabe Pharmaceutical Drug, Tokyo, Japan) (10 μg/mL) was added 72 h later, and the medium was collected and replaced with the same volume of fresh medium every 24 h. The concentration of MCP-1 in the medium collected from each well was determined by ELISA as described.[14]

***In vivo* studies in nude mice.** The following investigations were performed in accordance with the guidelines of our Institutional Animal Care and Use Committee. Six-week-old male athymic

[3]To whom correspondence should be addressed. E-mail: skaneko@m-kanazawa.jp

doi: 10.1111/j.1349-7006.2008.00951.x

nude mice (BALB/cA Jcl-nu; CLEA Japan, Tokyo, Japan) were injected subcutaneously with 1×10^7 HuH7 cells at the both sides of the flank on day 0. On days 3 and 4, 1×10^7 $TCID_{50}$ (100 μL) of Ad-tk, Ad-lacZ, or Ad-tk (1×10^7 $TCID_{50}$, fixed dose) plus Ad-MCP1 (1, 0.1, 0.01, or 0.001×10^7 $TCID_{50}$, changed dose) were injected into the tumor. Then, 75 mg/kg of GCV was administered into the peritoneal cavity daily for the next 5 consecutive days (day 5–9), and tumor size was measured every 3 days. Tumor volumes were calculated using the formula:

$$\frac{(\text{longest diameter}) \times (\text{shortest diameter})^2}{2}$$

Gene expression analysis (real-time reverse transcription–polymerase chain reaction [RT-PCR]). Total RNA was extracted from tumor tissues or spleens resected after treatment of the tumor with each rAd, using a Total Cellular RNA Isolation Kit (Ambion, St. Austin, TX, USA), in accordance with the manufacturer's protocol. The RNA was reverse transcribed with a TaqMan reverse transcription reagent kit (PE Applied Biosystems, Foster City, CA, USA) using random hexamer primers. Gene expression was analyzed by real-time RT-PCR using TaqMan Universal Master Mix on an ABI PRISM 7900 Sequence Detection System (PE Applied Biosystems). The PCR primer pairs for mouse interleukin (IL)–10, IL-12, IL-18, IFN-γ, VEGF, and 18S rRNA were obtained from the TaqMan assay reagent library. Data for whole samples were normalized to 18S rRNA and then expressed as the fold change in mRNA expression as compared with control samples treated with phosphate-buffered saline (PBS).

Immunohistochemical analysis. Tumor tissues were resected on day 10. The tissue samples were embedded in OCT compound (Sakura Finetek, Torrance, CA, USA) and snap-frozen in liquid nitrogen. Cryostat sections of frozen tissues were fixed in cold acetone for 10 min, followed by three rinses in PBS. To avoid non-specific staining, avidin and biotin in the tissues were blocked using a blocking kit (Vector Laboratories, Burlingame, CA, USA). The slides were subsequently incubated with antibodies (Abs) against Mac-1 (M1/70; Pharmingen, San Diego, CA, USA) for 30 min at room temperature. Negative controls included staining with non-specific Ab of the corresponding isotype and subsequent staining with secondary Ab. The reactions were visualized using a VECTASTAIN ABC Standard Kit (Vector Laboratories), followed by counterstaining with hematoxylin.

Preparation of peritoneal exudate macrophages and assays for cytokine production *in vitro*. Thioglycolate-elicited murine peritoneal exudate cells were collected as described.[15] Briefly, nude or immunocompetent mice were injected intraperitoneally with 2 mL each of 3% fluid thioglycolate medium (Wako Pure Chemical) and sacrificed 4 days later, followed by peritoneal lavage with 10 mL of cold PBS. About 90% of the collected peritoneal cells were positive for both Mac-1 (CD11b) and $I\text{-}A^d$ MHC class II as determined by staining with PE-conjugated anti-Mac-1 Ab and fluorescein-isothiocyanate (FITC)–conjugated $I\text{-}A^d$ MHC class II (AMS-32.1; Pharmingen). Huh7 cells were infected with rAds, at a MOI of 5 for 24 h. Aliquots of 10^5 macrophages were cocultured with 10^5 rAd-treated Huh7 cells in 1.0 mL of culture media in 24-well tissue culture plates, and treated with GCV for 2 days at 37°C. The concentrations of IL-10, IL-12, IL-18, and IFN-γ in the media were quantified using immunoassay kits (IL-10, IL-12, IFN-γ: Biosource International, Camarillo, CA, USA; IL-18: Medical & Biological Laboratories, Nagoya, Japan).

Rechallenge testing in nude mice. Nude mice were injected subcutaneously with 5×10^6 HuH7 cells on day 0. On days 3 and 4, the subcutaneous tumors were injected with 5×10^7 $TCID_{50}$ (100 μL) of Ad-tk, Ad-lacZ, or Ad-tk (fixed dose) plus Ad-MCP1 (changed dose), and the mice were treated with 75 mg/kg GCV, injected into the peritoneal cavity, every day for the next 5 days (days 5–9). Following complete eradication of the primary tumors, the mice were subcutaneously rechallenged on day 14 with 3×10^6 HuH7 cells at two sites, which were more than 3 cm apart from the primary challenge site. Two of 10 (20%) mice treated with Ad-tk and four of 30 (13.3%) treated with Ad-tk plus Ad-MCP1 did not show complete eradication of the primary tumor by the final measurement and were therefore excluded from the rechallenge experiment. Tumor sizes were measured every 4 days after the second tumor injection, and tumor volumes were calculated using the formula:

$$\frac{(\text{longest diameter}) \times (\text{shortest diameter})^2}{2}$$

Animal studies in immunocompetent mice (*ex vivo*, *in vivo*, and rechallenge). Six-week-old immunocompetent male BALB/c-jcl mice (CLEA Japan) were injected subcutaneously with 1×10^5 BNL cells infected with each rAd at an *in vitro* MOI of 5 at the both sides of the flank on day 0, and GCV was administered intraperitoneally for the next 5 days (days 1–5). Tumor size was measured every 7 days, and tumor volume was calculated using the formula:

$$\frac{(\text{longest diameter}) \times (\text{shortest diameter})^2}{2}$$

As with the experiments on nude mice, BALB/c-jcl mice were injected subcutaneously with 1×10^5 BNL cells at the both sides of the flank on day 0. On days 3 and 4, 5×10^5 $TCID_{50}$ (100 μL) of rAds were injected into the tumor. Then, GCV was administered for the next 5 days (day 5–9), and tumor size was measured every 3 days.

In another experiment, immunocompetent mice were injected subcutaneously with 1×10^5 BNL cells infected with each rAd at an *in vitro* MOI of 100 on day 0, and GCV was administered intraperitoneally for the next 5 days (days 1–5). The primary tumors were completely eradicated in all groups. These mice were injected subcutaneously with 1×10^4 BNL cells on day 14 at two sites which were separate from the primary challenge sites, and the tumor sizes were measured every 7 days after the second tumor injection.

ELISA for serum IL-10, IL-12, and IL-18. Mouse sera were collected prior to injection of subcutaneous primary tumors and on day 35 after tumor injection. IL-10, IL-12, and IL-18 concentrations were measured using immunoassay kits (IL-12, Biosource International; IL-18, Medical & Biological Laboratories).

Flow cytometry. Single-cell suspensions of splenocytes were resuspended in PBS containing 1% bovine serum albumin and 0.1% sodium azide, and incubated for 30 min on ice with FITC-conjugated rat antimouse-F4/80 (Serotec, Oxford, UK) and PE-conjugated rat antimouse pan natural killer (NK) cells (DX5; Pharmingen), with FITC-conjugated rat antimouse-CD3 (Pharmingen) and PE-conjugated rat antimouse CD11c (Pharmingen) or with FITC-conjugated rat antimouse-CD8 (Pharmingen) and PE-conjugated rat antimouse CD4 (Pharmingen). The cells were washed, resuspended in PBS, and analyzed using a FACScan with CellQuest software.

Statistical analysis. All results are expressed as means ± SE. The statistical significance of differences between groups was evaluated by the Mann–Whitney *U*-test.

Results

MCP-1 production by double infection with recombinant adenoviruses *in vitro*. MCP-1 expression level by Ad-MCP1 alone was high compared with double infection of Ad-lacZ plus Ad-MCP1 (Fig. 1a). The amounts of MCP-1 produced by Ad-tk plus Ad-MCP1 decreased rapidly after GCV administration due to Huh7 cell

doi: 10.1111/j.1349-7006.2008.00951.x

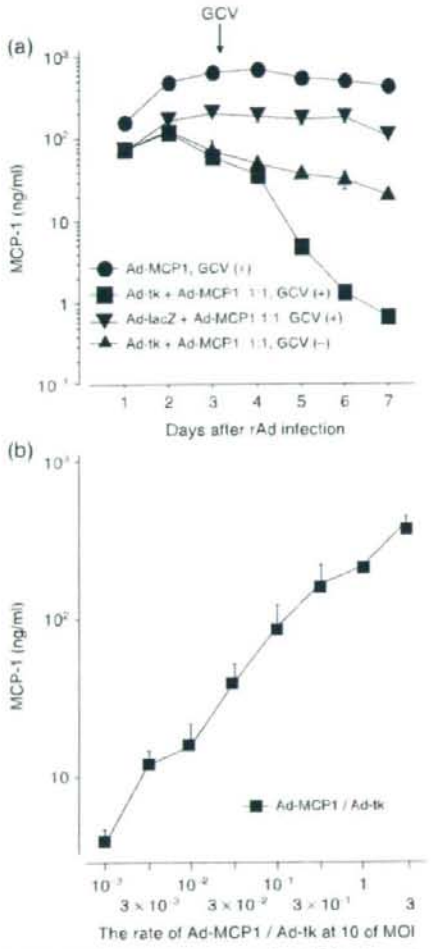

Fig. 1. Monocyte chemoattractant protein-1 (MCP-1) production of recombinant adenoviruses in the presence of herpes simplex virus thymidine kinase (HSV-tk). Aliquots of 1×10^5 Huh7 cells were seeded in 1.0 mL of culture media in 24-well tissue culture plates. (a) Twenty-four h later, the cells were treated with Ad-tk plus Ad-MCP1, Ad-lacZ plus Ad-MCP1, or Ad-MCP1 at a multiplicity of infection (MOI) of 10, and treated 72 h later with ganciclovir (GCV) (10 μg/mL). Every 24 h, the medium was collected and replaced with the same volume of fresh medium. (b) Twenty-four h later, the cells were doubly infected with Ad-tk (fixed dose, at an MOI of 10) plus Ad-MCP1 (changed dose), and the medium was collected 48 h later. The concentrations of MCP-1 were evaluated using an immunoassay. Values are shown as the means ± SE of duplicate experiments.

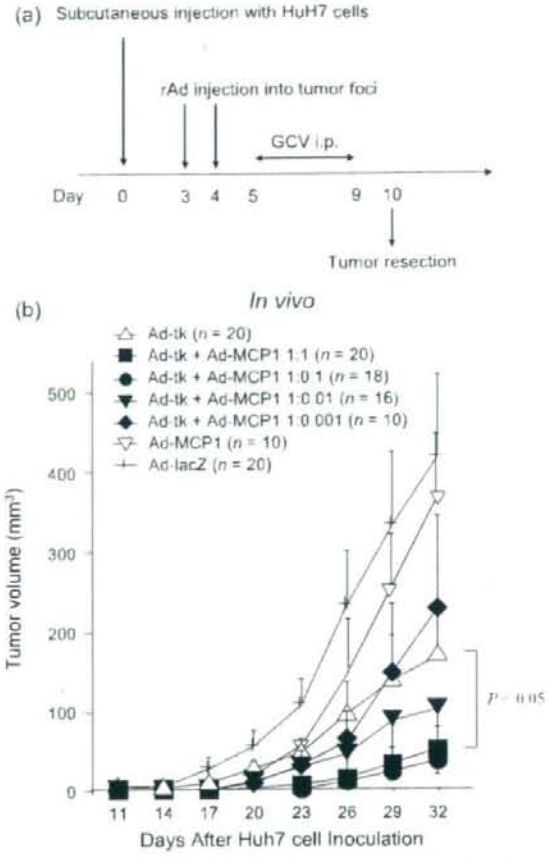

Fig. 2. The antitumor effects of the herpes simplex virus thymidine kinase (HSV-tk)/ganciclovir (GCV) system by codelivery of monocyte chemoattractant protein-1 (MCP-1) in a nude mouse model of hepatocellular carcinoma (HCC). (a) Mice were injected subcutaneously with 1×10^7 Huh7 cells at the both sides of the flank on day 0. On days 3 and 4, 1×10^7 $TCID_{50}$ of Ad-tk, Ad-tk (1×10^7 $TCID_{50}$, fixed dose) plus Ad-MCP1 (1, 0.1, 0.01, or 0.001×10^7 $TCID_{50}$, changed dose), or Ad-lacZ was injected into the tumor, and the mice were injected intraperitoneally (i.p.) with 75 mg/kg of GCV every day for the next 5 days (day 5–9). (b) Tumor size was measured every 3 days. The results are shown as the means of two independent experiments.

apoptosis induced by the HSV-tk/GCV system (Fig. 1a). Moreover, the amounts of MCP-1 produced by Ad-tk plus Ad-MCP1 without GCV administration were lower than those of Ad-lacZ plus Ad-MCP1, presumably due to the MCP-1 promoter interference by HSV-tk.

Next, production of MCP-1 in Huh7 cells double-infected with Ad-tk (fixed dose) plus Ad-MCP1 (changed dose) was measured. The amounts of MCP-1 were correlated with the infectious dose of Ad-MCP1 in the presence of a fixed amount of HSV-tk (Fig. 1b).

Antitumor effects of the HSV-tk/GCV system by codelivery of the *MCP-1* gene in an athymic nude mouse model of HCC. The *in vivo* antitumor effects of double infection with rAds were analyzed using athymic nude mice (Fig. 2a). The growth of subcutaneous tumors was markedly suppressed in animals treated with Ad-tk plus Ad-MCP1 (1:1) (tumor volume 32 days after injection, 44.4 ± 22.5 mm^3) or Ad-tk plus Ad-MCP1 (1:0.1) (37.4 ± 18.6 mm^3), as compared to those treated with Ad-tk alone (170.2 ± 49.8 mm^3, $P < 0.05$) (Fig. 2b). These observations indicated that optimal amounts of MCP-1 are needed to eradicate tumor cells in the presence of HSV-tk.

Recruitment and activation of macrophages into tumor tissues. Macrophages play important roles in both Th1- and Th2-mediated immune responses. Classical macrophage (M1 macrophages) are also a major source of IL-12 and IL-18, whereas alternative macrophages (M2 macrophages) are a source of IL-10.[9] IL-12

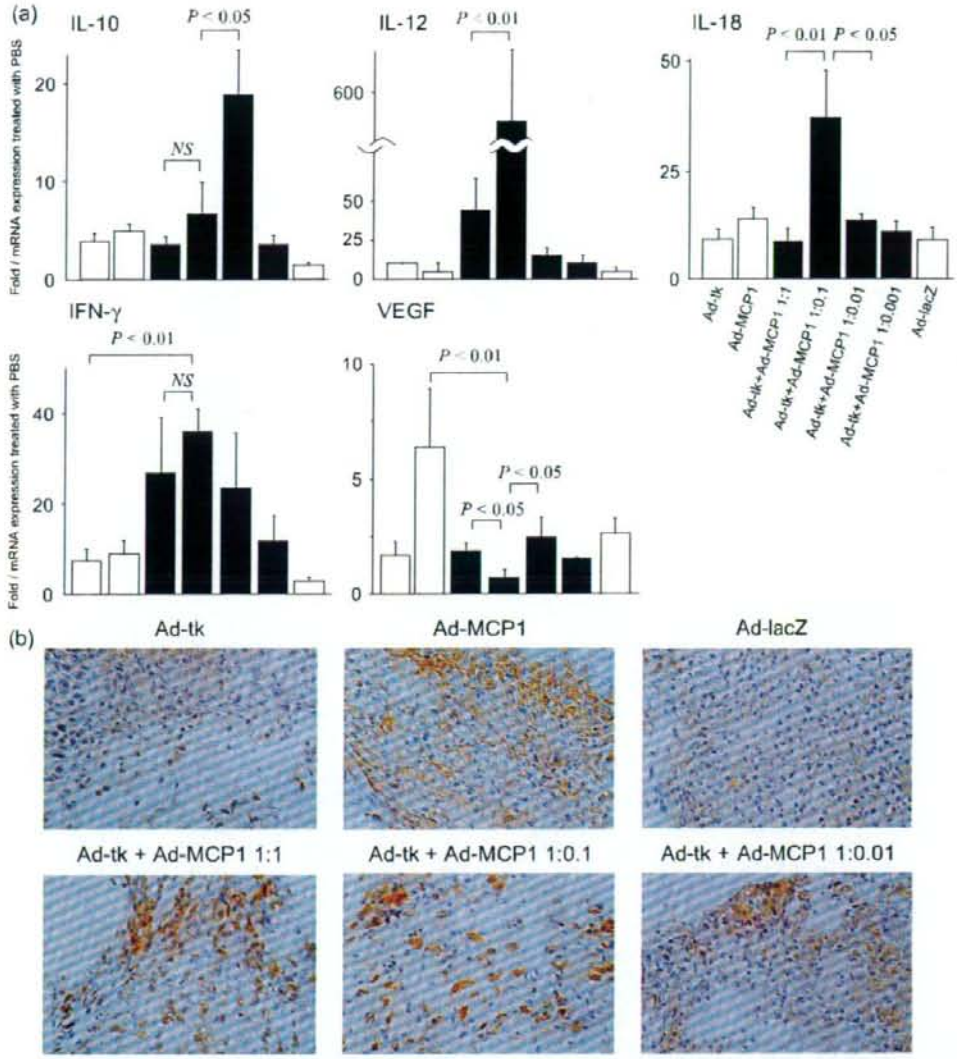

Fig. 3. Cytokine expression and macrophage recruitment in primary tumor tissues. In the experiment described in the legend to Fig. 2, tumor tissues were resected 10 days after tumor injection. (a) Total RNA was extracted to determine cytokine mRNA levels by a real-time reverse transcription–polymerase chain reaction as described in 'Materials and Methods'. Cytokine mRNA expression was normalized to 18S rRNA and then expressed as the fold change in mRNA expression as compared with control samples treated with phosphate-buffered saline. Splenocytes treated with 0.1 μg/mL LPS were used as a positive control (data not shown). The results are shown as the means of two independent experiments. (b) Tumor tissues were processed for immunohistochemical analysis using anti-Mac1 antibody as described in 'Materials and Methods'. Representative results from individual animals in each group are shown here.

enhances the activities of NK cells and cytotoxic T lymphocytes (CTL), and plays a key role in the induction of Th1-type immune responses.[16] In addition, IL-18 is a proinflammatory cytokine produced by activated macrophages, which has been shown to induce Th1 cell development and NK cell activation in combination with IL-12.[17] In contrast, the effects of IL-10 on immune responses are mostly inhibitory.[18] Therefore, to evaluate whether M1 macrophages recruited into tumor tissues following infection with rAds were activated, IL-10, IL-12, IL-18, IFN-γ, and VEGF expression were determined using real-time RT-PCR. IL-12 and IL-18 mRNA levels were significantly increased ($P < 0.01$), and that of IFN-γ mRNA tended to increase in tumors treated with Ad-tk plus Ad-MCP1 (1:0.1) (Fig. 3a). In contrast, IL-10 mRNA was significantly increased in tumors treated with Ad-tk plus Ad-MCP1 (1:0.01) ($P < 0.05$) (Fig. 3a). In addition, the VEGF mRNA level was significantly increased in tumors treated with Ad-MCP1 ($P < 0.01$), and was significantly decreased in tumors treated with Ad-tk plus Ad-MCP1 (1:0.1)

doi: 10.1111/j.1349-7006.2008.00951.x

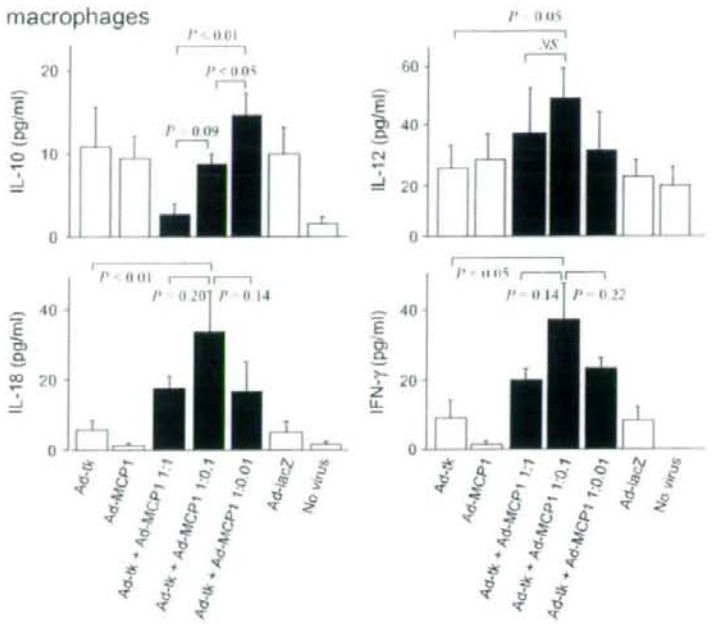

Fig. 4. Cytokine production by peritoneal macrophages cocultured with Huh7 cells infected with rAds *in vitro*. Huh7 cells were infected with each rAd at a multiplicity of infection (MOI) of 5 and treated with ganciclovir (GCV) for 24 h. Aliquots of 10^5 peritoneal exudate macrophages were cocultured with 10^5 rAd-treated Huh7 cells for 2 days, and the concentrations of IL-10, IL-12, IL-18, and IFN-γ in the media were evaluated by immunoassay. Values are shown as the means ± SE of duplicate experiments.

($P < 0.05$) (Fig. 3a). Taken together, these observations indicated that M1 macrophages were highly activated when tumors were treated with the optimal dose of MCP-1 and HSV-tk.

Next, we evaluated whether there were differences in the number of macrophages recruited into tumor tissues. The number of accumulated Mac-1-positive cells in the tumors treated with Ad-tk plus Ad-MCP1 (1:0.1) was comparable to that in those treated with Ad-tk plus Ad-MCP1 (1:1) (Fig. 3b). These observations suggested that the number of recruited macrophages is of little importance to the antitumor effects.

IL-10, IL-12, IL-18, and IFN-γ production by coculture of apoptotic Huh7 cells expressing MCP-1 and peritoneal macrophages *in vitro*. It was reported that adenoviral-mediated overexpression of MCP-1 differentially modulated the development of Th1 and Th2-type responses.[19] To evaluate the differences in the immunomodulatory effects of macrophages among double infection of rAds, we measured IL-10, IL-12, IL-18, and IFN-γ production by peritoneal exudate cells consisting mostly of macrophages, when they were cocultured with Huh7 cells infected with rAds. We found that peritoneal macrophages cocultured with Huh7 cells treated with Ad-tk plus Ad-MCP1 (1:0.1) tended to produce increased levels of IL-12, IL-18, and IFN-γ (Fig. 4). On the other hand, the increase in amount of IL-10 in the double infection groups was inversely proportional to the dosage of MCP-1 vector (Fig. 4). These observations also suggest that the optimal dose of MCP-1 and HSV-tk may induce M1 macrophage activation.

Antitumor immunity in the rechallenge test of the HSV-tk/GCV system by codelivery of the *MCP-1* gene. After primary subcutaneous Huh7 cells were completely eradicated with rAds, nude mice were rechallenged with Huh7 cells to evaluate antitumor immunity induced by MCP-1 plus HSV-tk. We found that the tumor regrowth was significantly suppressed when the primary tumor cells had been eradicated with Ad-tk plus Ad-MCP1 (1:0.1) as compared with Ad-tk (tumor volume 40 days after rechallenge: 123.2 ± 77.2 mm^3 *vs* 544.5 ± 161.6 mm^3, respectively, $P < 0.05$) (Fig. 5). In addition, tumor regrowth tended to be low when eradicated with Ad-tk plus Ad-MCP1 (1:0.1) as compared with Ad-tk plus Ad-MCP1 (1:1) (287.9 ± 137.1 mm^3, $P = 0.18$) or Ad-tk plus Ad-MCP1 (1:0.01) (269.7 ± 91.1 mm^3, $P = 0.24$). Next, to evaluate immunomodulatory effects of splenocytes, we examined IFN-γ expression using real-time RT-PCR. IFN-γ mRNA levels were significantly increased in the spleens of nude mice treated with Ad-tk plus Ad-MCP1 (1:0.1) (Fig. 5b). Consistent with our previous findings,[20] we observed increased numbers of NK cells in the spleen and rechallenged tumor tissues when treated with the 1:0.1 ratio of Ad-tk and Ad-MCP1 (data not shown). These results indicated that the optimal dose of MCP-1 induced beneficial antitumor immunity in the presence of HSV-tk.

Antitumor effects and immunity of the HSV-tk/GCV system plus MCP-1 treatment in an immunocompetent mouse model of HCC. There is no CTL in athymic nude mice. Therefore, to evaluate the Th1 cytokine response in the syngeneic system, the *ex vivo* antitumor effects of double infection with rAds were analyzed using immunocompetent BALB/c-jcl mice. The growth of subcutaneous tumors treated with Ad-tk plus Ad-MCP1 (1:1, 1:0.1) was comparable to that in nude mice ($P < 0.01$), excluding the group in which the dose of MCP-1 was small (1:0.01) (Fig. 6a).

In the next experiment, after the BALB/c mice developed tumor mass following the injection with non-infected BNL cells, we infected the resultant tumors with Ad-tk plus Ad-MCP1 and treated the animals with GCV using the same procedures as the experiments with nude mice. Tumor growth was apparently retarded when treated with Ad-tk plus Ad-MCP1 (1:1) ($P < 0.05$) and (1:0.1) ($P < 0.01$) as compared with Ad-tk alone (Fig. 6b). However, the treatments failed to eradicate tumors completely, probably because the infection efficiency was not sufficient under these conditions.

Thus, we chose the *ex vivo* infection experiment in the immunocompetent mouse model, to evaluate whether rechallenged tumors could be rejected in the mice in which the primary tumors had been completely eradicated. The immunocompetent mice were rechallenged with BNL 1ME A.7R.1 (BNL) cells

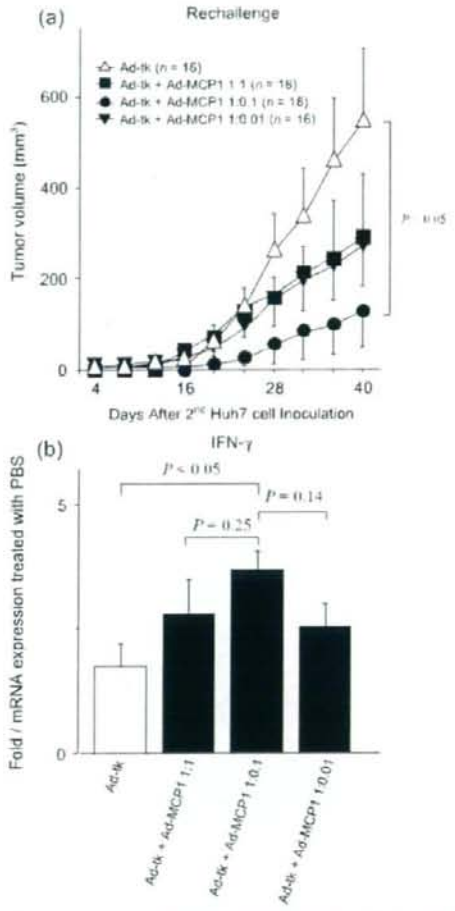

Fig. 5. Nude mice were injected subcutaneously with 5×10^6 Huh7 cells on day 0. On days 3 and 4, 5×10^7 $TCID_{50}$ of Ad-tk (100 μL), Ad-tk (1×10^7 $TCID_{50}$, fixed dose) plus Ad-MCP1 (1, 0.1, 0.01, or 0.001×10^7 $TCID_{50}$, changed dose), or Ad-lacZ was injected into the tumor, and the mice were injected intraperitoneally with 75 mg/kg of ganciclovir (GCV) every day for the next 5 days (day 5–9). Following complete eradication of the primary tumors, the mice were subcutaneously rechallenged on day 14 with 3×10^6 Huh7 cells at the other sites. (a) Tumor size was measured every 4 days. (b) In another series of experiments, the spleen was resected on day 16 after tumor injection, and IFN-γ, mRNA levels were evaluated using real-time reverse transcription–polymerase chain reaction. The results are shown as the means of two independent experiments. PBS, phosphate-buffered saline.

using the same procedures as in the experiments with nude mice. Although the inhibition of tumor regrowth was significantly lower when they had been eradicated with Ad-tk plus Ad-MCP1 (1:0.1) as compared with Ad-tk (tumor volume 42 days after rechallenge: 263.9 ± 87.8 mm^3 *vs* 669.5 ± 158.3 mm^3, respectively, $P < 0.05$), it also tended to be lower when the primary tumor cells had been eradicated with Ad-tk plus Ad-MCP1 (1:1) (tumor volume 42 days after rechallenge: 372.5 ± 157.8 mm^3) (Fig. 6c), similar to the observations in athymic nude mice.

Next, we examined IL-10, IL-12, and IL-18 production on day 35 after tumor injection. Serum concentrations of IL-12 and IL-18 tended to be higher in mice treated with Ad-tk plus Ad-MCP1 (1:0.1) as compared with those treated with Ad-tk, Ad-tk plus Ad-MCP1 (1:1), or Ad-tk plus Ad-MCP1 (1:0.01) (Fig. 6d). In contrast, the increase in amount of serum IL-10 in the double infection groups was inversely proportional to the dosage of MCP-1 (Fig. 6d). These observations were consistent with the data shown in Figs 3 and 4.

Finally, to monitor the activation state of innate and acquired immunity in extrahepatic lymphoid organs, we examined the numbers of immune cells in the spleen on day 35 after tumor injection by FACS analysis. The numbers of F4/80-positive cells tended to be higher in the Ad-tk plus Ad-MCP1 (1:1) and Ad-tk plus Ad-MCP1 (1:0.1) groups, and the numbers of DX5-positive cells tended to be higher in the Ad-tk plus Ad-MCP1 (1:0.1) group (Fig. 6e). Furthermore, the numbers of CD3-, CD4-, and CD8-positive cells were increased in the immunocompetent mice in the order of Ad-tk plus Ad-MCP1 (1:0.1), Ad-tk plus Ad-MCP1 (1:1), and Ad-tk plus Ad-MCP1 (1:0.01) (Fig. 6e). Taken together, these results confirmed that treatment with Ad-tk plus Ad-MCP1 (1:0.1) resulted in the development of beneficial antitumor immunity in both immunodeficient and immunocompetent animals.

Discussion

HCC is one of the most common cancer-related causes of death, and is resistant to anticancer drugs.[21] Although gene therapy has the potential to more effectively induce tumor cell death as compared to conventional treatment, there have been no previous comparisons with regard to the optimal doses of vectors in combined gene therapy. Whereas the amounts of MCP-1 were correlated with the infectious dose of Ad-MCP1 in the presence of a fixed dose of Ad-tk, MCP-1 expression level in the presence of intracellular HSV-tk was inhibited as compared with coinfection with Ad-MCP1 plus Ad-lacZ, suggesting that HSV-tk may influence the efficiency of transcription in the transformed cells. In addition, MCP-1 expression level by Ad-MCP1 alone was high as compared with double infection with Ad-MCP1 plus Ad-lacZ, which was probably due to promoter interference. On the other hand, our previous study demonstrated that the levels of HSV-tk expression in cells cotransfected with Ad-tk plus Ad-MCP-1 were comparable to those of Ad-tk alone or Ad-tk plus Ad-lacZ.[3] The effect of a bicistronic rAd expressing mainly HSV-tk was clearly stronger than that of a bicistronic rAd expressing mainly MCP-1. Therefore, we proposed that the

Fig. 6. Antitumor effects of the herpes simplex virus thymidine kinase (HSV-tk)/ganciclovir (GCV) system by codelivery of monocyte chemoattractant protein-1 (MCP-1) in an immunocompetent mouse model of HCC. (a) Mice were injected subcutaneously with 1×10^5 BNL cells infected with each rAd at an *in vitro* multiplicity of infection (MOI) of 5 at the both sides of the flank on day 0. GCV was administered intraperitoneally for the next 5 days (days 1–5), and tumor size was measured every 7 days. (b) BALB/c-jcl mice were injected subcutaneously with 1×10^5 BNL cells at the both sides of the flank on day 0. On days 3 and 4, 5×10^5 $TCID_{50}$ (100 μL) of rAds were injected into the tumor. Then, GCV was administered for the next 5 days (day 5–9), and tumor size was measured every 3 days. (c) BALB/c-jcl mice were injected subcutaneously with 1×10^5 BNL cells infected with each rAd at an *in vitro* MOI of 100 on day 0, and GCV was administered intraperitoneally for the next 5 days (days 1–5). The primary tumors were completely eradicated in all groups. These mice were injected subcutaneously with 1×10^4 BNL cells at other sites on day 14, and the tumor sizes were measured every 7 days after the second tumor injection. (d) Mouse sera were collected prior to subcutaneous injection of primary tumor cells (untreated), after treatment of the tumor with each rAd, and 2 days after rechallenge with HuH7 cells, and IL-12 and IL-18 concentrations were measured using immunoassay kits. (e) The spleen was removed to obtain single cell suspensions on day 35 after tumor injection. Surface expression of DX5, F4/80, CD3, CD4, CD8, and CD11c in cell populations obtained from the spleen were assessed by FACS. The results are representative of two independent experiments.

doi: 10.1111/j.1349-7006.2008.00951.x

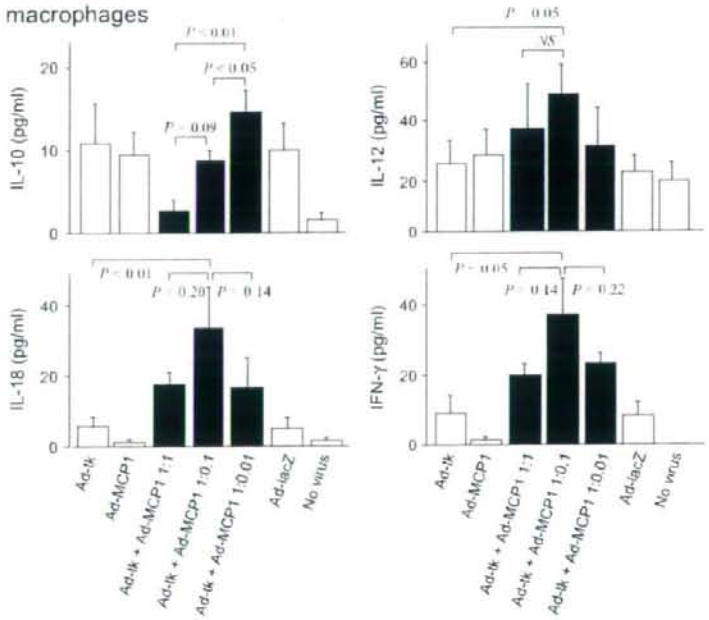

Fig. 4. Cytokine production by peritoneal macrophages cocultured with Huh7 cells infected with rAds *in vitro*. Huh7 cells were infected with each rAd at a multiplicity of infection (MOI) of 5 and treated with ganciclovir (GCV) for 24 h. Aliquots of 10^5 peritoneal exudate macrophages were cocultured with 10^5 rAd-treated Huh7 cells for 2 days, and the concentrations of IL-10, IL-12, IL-18, and IFN-γ in the media were evaluated by immunoassay. Values are shown as the means ± SE of duplicate experiments.

($P < 0.05$) (Fig. 3a). Taken together, these observations indicated that M1 macrophages were highly activated when tumors were treated with the optimal dose of MCP-1 and HSV-tk.

Next, we evaluated whether there were differences in the number of macrophages recruited into tumor tissues. The number of accumulated Mac-1-positive cells in the tumors treated with Ad-tk plus Ad-MCP1 (1:0.1) was comparable to that in those treated with Ad-tk plus Ad-MCP1 (1:1) (Fig. 3b). These observations suggested that the number of recruited macrophages is of little importance to the antitumor effects.

IL-10, IL-12, IL-18, and IFN-γ production by coculture of apoptotic Huh7 cells expressing MCP-1 and peritoneal macrophages *in vitro*. It was reported that adenoviral-mediated overexpression of MCP-1 differentially modulated the development of Th1 and Th2-type responses.[19] To evaluate the differences in the immunomodulatory effects of macrophages among double infection of rAds, we measured IL-10, IL-12, IL-18, and IFN-γ production by peritoneal exudate cells consisting mostly of macrophages, when they were cocultured with Huh7 cells infected with rAds. We found that peritoneal macrophages cocultured with Huh7 cells treated with Ad-tk plus Ad-MCP1 (1:0.1) tended to produce increased levels of IL-12, IL-18, and IFN-γ (Fig. 4). On the other hand, the increase in amount of IL-10 in the double infection groups was inversely proportional to the dosage of MCP-1 vector (Fig. 4). These observations also suggest that the optimal dose of MCP-1 and HSV-tk may induce M1 macrophage activation.

Antitumor immunity in the rechallenge test of the HSV-tk/GCV system by codelivery of the *MCP-1* gene. After primary subcutaneous Huh7 cells were completely eradicated with rAds, nude mice were rechallenged with Huh7 cells to evaluate antitumor immunity induced by MCP-1 plus HSV-tk. We found that the tumor regrowth was significantly suppressed when the primary tumor cells had been eradicated with Ad-tk plus Ad-MCP1 (1:0.1) as compared with Ad-tk (tumor volume 40 days after rechallenge: 123.2 ± 77.2 mm^3 *vs* 544.5 ± 161.6 mm^3, respectively, $P < 0.05$) (Fig. 5). In addition, tumor regrowth tended to be low when eradicated with Ad-tk plus Ad-MCP1 (1:0.1) as compared with Ad-tk plus Ad-MCP1 (1:1) (287.9 ± 137.1 mm^3, $P = 0.18$) or Ad-tk plus Ad-MCP1 (1:0.01) (269.7 ± 91.1 mm^3, $P = 0.24$). Next, to evaluate immunomodulatory effects of splenocytes, we examined IFN-γ expression using real-time RT-PCR. IFN-γ mRNA levels were significantly increased in the spleens of nude mice treated with Ad-tk plus Ad-MCP1 (1:0.1) (Fig. 5b). Consistent with our previous findings,[20] we observed increased numbers of NK cells in the spleen and rechallenged tumor tissues when treated with the 1:0.1 ratio of Ad-tk and Ad-MCP1 (data not shown). These results indicated that the optimal dose of MCP-1 induced beneficial antitumor immunity in the presence of HSV-tk.

Antitumor effects and immunity of the HSV-tk/GCV system plus MCP-1 treatment in an immunocompetent mouse model of HCC. There is no CTL in athymic nude mice. Therefore, to evaluate the Th1 cytokine response in the syngeneic system, the *ex vivo* antitumor effects of double infection with rAds were analyzed using immunocompetent BALB/c-jcl mice. The growth of subcutaneous tumors treated with Ad-tk plus Ad-MCP1 (1:1, 1:0.1) was comparable to that in nude mice ($P < 0.01$), excluding the group in which the dose of MCP-1 was small (1:0.01) (Fig. 6a).

In the next experiment, after the BALB/c mice developed tumor mass following the injection with non-infected BNL cells, we infected the resultant tumors with Ad-tk plus Ad-MCP1 and treated the animals with GCV using the same procedures as the experiments with nude mice. Tumor growth was apparently retarded when treated with Ad-tk plus Ad-MCP1 (1:1) ($P < 0.05$) and (1:0.1) ($P < 0.01$) as compared with Ad-tk alone (Fig. 6b). However, the treatments failed to eradicate tumors completely, probably because the infection efficiency was not sufficient under these conditions.

Thus, we chose the *ex vivo* infection experiment in the immunocompetent mouse model, to evaluate whether rechallenged tumors could be rejected in the mice in which the primary tumors had been completely eradicated. The immunocompetent mice were rechallenged with BNL 1ME A.7R.1 (BNL) cells

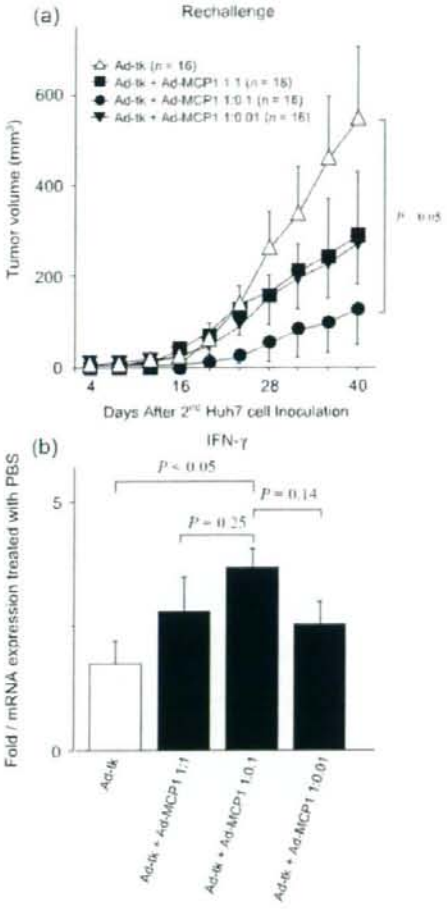

Fig. 5. Nude mice were injected subcutaneously with 5×10^6 Huh7 cells on day 0. On days 3 and 4, 5×10^7 $TCID_{50}$ of Ad-tk (100 μL), Ad-tk (1×10^7 $TCID_{50}$, fixed dose) plus Ad-MCP1 (1, 0.1, 0.01, or 0.001×10^7 $TCID_{50}$, changed dose), or Ad-lacZ was injected into the tumor, and the mice were injected intraperitoneally with 75 mg/kg of ganciclovir (GCV) every day for the next 5 days (day 5–9). Following complete eradication of the primary tumors, the mice were subcutaneously rechallenged on day 14 with 3×10^6 Huh7 cells at the other sites. (a) Tumor size was measured every 4 days. (b) In another series of experiments, the spleen was resected on day 16 after tumor injection, and IFN-γ, mRNA levels were evaluated using real-time reverse transcription–polymerase chain reaction. The results are shown as the means of two independent experiments. PBS, phosphate-buffered saline.

using the same procedures as in the experiments with nude mice. Although the inhibition of tumor regrowth was significantly lower when they had been eradicated with Ad-tk plus Ad-MCP1 (1:0.1) as compared with Ad-tk (tumor volume 42 days after rechallenge: 263.9 ± 87.8 mm³ *vs* 669.5 ± 158.3 mm³, respectively, $P < 0.05$), it also tended to be lower when the primary tumor cells had been eradicated with Ad-tk plus Ad-MCP1 (1:1) (tumor volume 42 days after rechallenge: 372.5 ± 157.8 mm³) (Fig. 6c), similar to the observations in athymic nude mice.

Next, we examined IL-10, IL-12, and IL-18 production on day 35 after tumor injection. Serum concentrations of IL-12 and IL-18 tended to be higher in mice treated with Ad-tk plus Ad-MCP1 (1:0.1) as compared with those treated with Ad-tk, Ad-tk plus Ad-MCP1 (1:1), or Ad-tk plus Ad-MCP1 (1:0.01) (Fig. 6d). In contrast, the increase in amount of serum IL-10 in the double infection groups was inversely proportional to the dosage of MCP-1 (Fig. 6d). These observations were consistent with the data shown in Figs 3 and 4.

Finally, to monitor the activation state of innate and acquired immunity in extrahepatic lymphoid organs, we examined the numbers of immune cells in the spleen on day 35 after tumor injection by FACS analysis. The numbers of F4/80-positive cells tended to be higher in the Ad-tk plus Ad-MCP1 (1:1) and Ad-tk plus Ad-MCP1 (1:0.1) groups, and the numbers of DX5-positive cells tended to be higher in the Ad-tk plus Ad-MCP1 (1:0.1) group (Fig. 6e). Furthermore, the numbers of CD3-, CD4-, and CD8-positive cells were increased in the immunocompetent mice in the order of Ad-tk plus Ad-MCP1 (1:0.1), Ad-tk plus Ad-MCP1 (1:1), and Ad-tk plus Ad-MCP1 (1:0.01) (Fig. 6e). Taken together, these results confirmed that treatment with Ad-tk plus Ad-MCP1 (1:0.1) resulted in the development of beneficial antitumor immunity in both immunodeficient and immunocompetent animals.

Discussion

HCC is one of the most common cancer-related causes of death, and is resistant to anticancer drugs.[21] Although gene therapy has the potential to more effectively induce tumor cell death as compared to conventional treatment, there have been no previous comparisons with regard to the optimal doses of vectors in combined gene therapy. Whereas the amounts of MCP-1 were correlated with the infectious dose of Ad-MCP1 in the presence of a fixed dose of Ad-tk, MCP-1 expression level in the presence of intracellular HSV-tk was inhibited as compared with coinfection with Ad-MCP1 plus Ad-lacZ, suggesting that HSV-tk may influence the efficiency of transcription in the transformed cells. In addition, MCP-1 expression level by Ad-MCP1 alone was high as compared with double infection with Ad-MCP1 plus Ad-lacZ, which was probably due to promoter interference. On the other hand, our previous study demonstrated that the levels of HSV-tk expression in cells cotransfected with Ad-tk plus Ad-MCP-1 were comparable to those of Ad-tk alone or Ad-tk plus Ad-lacZ.[3] The effect of a bicistronic rAd expressing mainly HSV-tk was clearly stronger than that of a bicistronic rAd expressing mainly MCP-1. Therefore, we proposed that the

Fig. 6. Antitumor effects of the herpes simplex virus thymidine kinase (HSV-tk)/ganciclovir (GCV) system by codelivery of monocyte chemoattractant protein-1 (MCP-1) in an immunocompetent mouse model of HCC. (a) Mice were injected subcutaneously with 1×10^5 BNL cells infected with each rAd at an *in vitro* multiplicity of infection (MOI) of 5 at the both sides of the flank on day 0. GCV was administered intraperitoneally for the next 5 days (days 1–5), and tumor size was measured every 7 days. (b) BALB/c-jcl mice were injected subcutaneously with 1×10^5 BNL cells at the both sides of the flank on day 0. On days 3 and 4, 5×10^5 $TCID_{50}$ (100 μL) of rAds were injected into the tumor. Then, GCV was administered for the next 5 days (day 5–9), and tumor size was measured every 3 days. (c) BALB/c-jcl mice were injected subcutaneously with 1×10^5 BNL cells infected with each rAd at an *in vitro* MOI of 100 on day 0, and GCV was administered intraperitoneally for the next 5 days (days 1–5). The primary tumors were completely eradicated in all groups. These mice were injected subcutaneously with 1×10^4 BNL cells at other sites on day 14, and the tumor sizes were measured every 7 days after the second tumor injection. (d) Mouse sera were collected prior to subcutaneous injection of primary tumor cells (untreated), after treatment of the tumor with each rAd, and 2 days after rechallenge with HuH7 cells, and IL-12 and IL-18 concentrations were measured using immunoassay kits. (e) The spleen was removed to obtain single cell suspensions on day 35 after tumor injection. Surface expression of DX5, F4/80, CD3, CD4, CD8, and CD11c in cell populations obtained from the spleen were assessed by FACS. The results are representative of two independent experiments.

doi: 10.1111/j.1349-7006.2008.00951.x

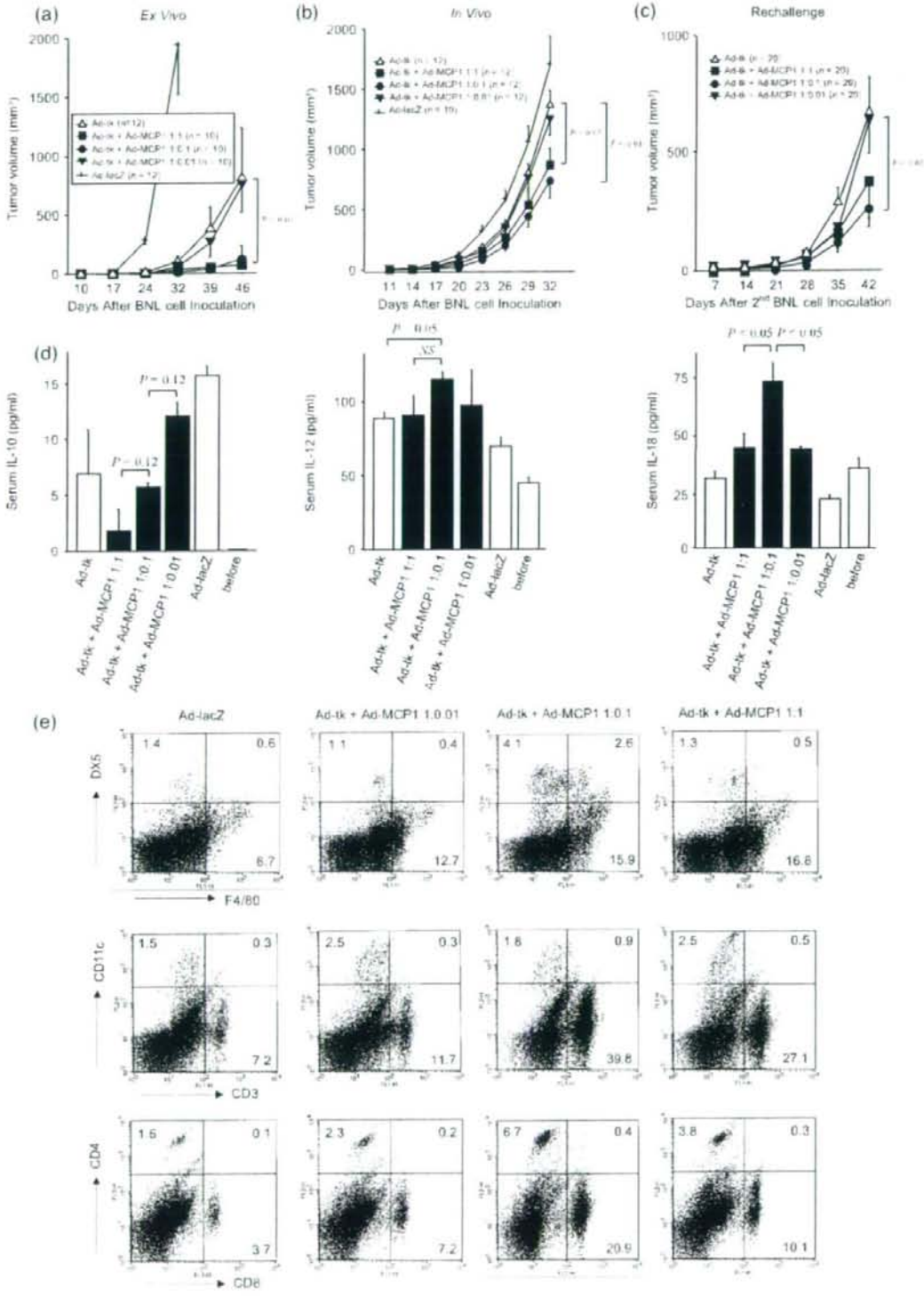

HSV-tk/GCV system should mainly be used and the use of MCP-1 was supported in our experimental models, although their efficiencies may vary depending on the nature of the cell type and reporter genes used.[22]

Th1 cytokine expression levels in tumors treated with Ad-tk plus Ad-MCP1 (1:0.1) were higher than those treated with Ad-tk plus Ad-MCP1 (1:1) or (1:0.01). Moreover, macrophages produced large amounts of Th1 cytokines when cocultured with apoptotic HCC cells induced by Ad-tk plus Ad-MCP1 (1:0.1). In contrast, whereas the amounts of Th2 cytokines were relatively high in Ad-tk plus Ad-MCP1 (1:0.01), they were low in Ad-tk plus Ad-MCP1 (1:1). There were almost no differences in the number of macrophages among the tumors treated with various combinations of HSV-tk and MCP-1. Therefore, the types of activated macrophages may be important rather than the numbers recruited and activated. The ratio of IL-12 to IL-10 can be used as a simple metric to classify activated macrophages into two categories, M1 or M2.[23,24] M1 macrophages are potent effector cells that kill microorganisms and tumor cells and produce large amounts of proinflammatory cytokines, particularly IL-12. In contrast, M2 macrophages, a producer of IL-10, tune inflammatory responses and adaptive Th1 immunity, scavenge debris, and promote angiogenesis, tissue remodeling, and repair. The M1/M2 dichotomy of macrophage polarization can elicit both anti- and pro-tumoral activities.[25]

MCP-1 is known to facilitate tumor growth under different conditions, probably by promoting angiogenesis.[8] In the present study, the VEGF expression levels in tumors treated with Ad-tk plus Ad-MCP1 (1:0.1) were low as compared with those treated with Ad-MCP1 alone or Ad-tk plus Ad-MCP1 (1:1 and 1:0.01). A previous study indicated that monocyte recruitment is dependent on the level of MCP-1 secreted by the tumor cells and that the effects of monocyte infiltration on tumor growth are dependent on their levels of infiltration.[26] MCP-1 secreted by apoptotic Huh7 cells may have recruited macrophages more efficiently to these apoptotic cells, thereby resulting in a greater deleterious effect on tumor formation. Therefore, we propose that it is necessary to set the appropriate dosages of the two vectors in the HSV-tk plus MCP-1 system.

Recently, we found that the HSV-tk/GCV system, together with delivery of MCP-1, eradicated HCC and exerted prolonged antitumor effects by activating macrophages and NK cells.[20] In this study, the antitumor immunity increased in mice treated with Ad-tk plus Ad-MCP1 (1:0.1). Several investigators have reported that dying HSV-tk-modified cells released soluble factors, including cytokines.[27,28] These factors could in turn affect the tumor microenvironment, leading to necrosis and inflammation, infiltration of immune cells, up-regulation of costimulatory molecules, and generation of an antitumorigenic immune responses.[28,29] In this immunotherapeutically favorable setting, the optimal dose of MCP-1 with HSV-tk inside the same cell may stimulate tumor-specific immune-mediated cell killing. Consequently, the delivery of an optimal amount of rAd expressing MCP-1 enhanced the antitumor effects of the HSV-tk/GCV system in a model of HCC, and the effects were related to the balance of Th1 and Th2–type cytokines.

References

1 Okada H, Miyamura K, Itoh T *et al.* Gene therapy against an experimental glioma using adeno-associated virus vectors. *Gene Ther* 1996; **3**: 957–64.
2 Coll JL, Mesnil M, Lefebvre MF, Lancon A, Favrot MC. Long-term survival of immunocompetent rats with intraperitoneal colon carcinoma tumors using herpes simplex thymidine kinase/ganciclovir and IL-2 treatments. *Gene Ther* 1997; **4**: 1160–6.
3 Tsuchiyama T, Kaneko S, Nakamoto Y *et al.* Enhanced antitumor effects of a bicistronic adenovirus vector expressing both herpes simplex virus thymidine kinase and monocyte chemoattractant protein-1 against hepatocellular carcinoma. *Cancer Gene Ther* 2003; **10**: 260–9.
4 Kagaya T, Nakamoto Y, Sakai Y *et al.* Monocyte chemoattractant protein-1 gene delivery enhances antitumor effects of herpes simplex virus thymidine kinase/ganciclovir system in a model of colon cancer. *Cancer Gene Ther* 2006; **13**: 357–66.
5 Matsushima K, Larsen CG, DuBois GC, Oppenheim JJ. Purification and characterization of a novel monocyte chemotactic and activating factor produced by a human myelomonocytic cell line. *J Exp Med* 1989; **169**: 1485–90.
6 Rollins BJ, Sunday ME. Suppression of tumor formation *in vivo* by expression of the JE gene in malignant cells. *Mol Cell Biol* 1991; **11**: 3125–31.
7 Nokihara H, Yanagawa H, Nishioka Y *et al.* Natural killer cell-dependent suppression of systemic spread of human lung adenocarcinoma cells by monocyte chemoattractant protein-1 gene transfection in severe combined immunodeficient mice. *Cancer Res* 2000; **60**: 7002–7.
8 Ueno T, Toi M, Saji H *et al.* Significance of macrophage chemoattractant protein-1 in macrophage recruitment, angiogenesis, and survival in human breast cancer. *Clin Cancer Res* 2000; **6**: 3282–9.
9 Mantovani A, Sozzani S, Locati M, Allavena P, Sica A. Macrophage polarization: tumor-associated macrophages as a paradigm for polarized M2 mononuclear phagocytes. *Trends Immunol* 2002; **23**: 549–55.
10 Kijima T, Osaki T, Nishino K *et al.* Application of the Cre recombinase/loxP system further enhances antitumor effects in cell type-specific gene therapy against carcinoembryonic antigen-producing cancer. *Cancer Res* 1999; **59**: 4906–11.
11 Freund CT, Sutton MA, Dang T, Contant CF, Rowley D, Lerner SP. Adenovirus-mediated combination suicide and cytokine gene therapy for bladder cancer. *Anticancer Res* 2000; **20**: 1359–65.
12 Sakai Y, Kaneko S, Sato Y *et al.* Gene therapy for hepatocellular carcinoma using two recombinant adenovirus vectors with alpha-fetoprotein promoter and Cre/lox P system. *J Virol Meth* 2001; **92**: 5–17.
13 Sato Y, Tanaka K, Lee G *et al.* Enhanced and specific gene expression via tissue-specific production of Cre recombinase using adenovirus vector. *Biochem Biophys Res Commun* 1998; **244**: 455–62.
14 Sakai Y, Kaneko S, Nakamoto Y, Kagaya T, Mukaida N, Kobayashi K. Enhanced anti-tumor effects of herpes simplex virus thymidine kinase/ganciclovir system by codelivering monocyte chemoattractant protein-1 in hepatocellular carcinoma. *Cancer Gene Ther* 2001; **8**: 695–704.
15 Kawaguchi T, Suematsu M, Koizumi HM *et al.* Activation of macrophage function by intraperitoneal administration of the streptococcal antitumor agent OK-432. *Immunopharmacology* 1983; **6**: 177–89.
16 Lamont AG, Adorini L. IL-12: a key cytokine in immune regulation. *Immunol Today* 1996; **17**: 214–7.
17 Okamura H, Kashiwamura S, Tsutsui H, Yoshimoto T, Nakanishi K. Regulation of interferon-gamma production by IL-12 and IL-18. *Curr Opin Immunol* 1998; **10**: 259–64.
18 Moore KW, de Waal Malefyt R, Coffman RL, O'Garra A. Interleukin-10 and the interleukin-10 receptor. *Annu Rev Immunol* 2001; **19**: 683–765.
19 Matsukawa A, Lukacs NW, Standiford TJ, Chensue SW, Kunkel SL. Adenoviral-mediated overexpression of monocyte chemoattractant protein-1 differentially alters the development of Th1 and Th2 type responses in vivo. *J Immunol* 2000; **164**: 1699–704.
20 Tsuchiyama T, Nakamoto Y, Sakai Y *et al.* Prolonged, NK cell-mediated antitumor effects of suicide gene therapy combined with monocyte chemoattractant protein-1 against hepatocellular carcinoma. *J Immunol* 2007; **178**: 574–83.
21 Okita K. Management of hepatocellular carcinoma in Japan. *J Gastroenterol* 2006; **41**: 100–6.
22 Mizuguchi H, Xu Z, Ishii-Watabe A, Uchida E, Hayakawa T. IRES-dependent second gene expression is significantly lower than cap-dependent first gene expression in a bicistronic vector. *Mol Ther* 2000; **1**: 376–82.
23 Mantovani A, Sica A, Sozzani S, Allavena P, Vecchi A, Locati M. The chemokine system in diverse forms of macrophage activation and polarization. *Trends Immunol* 2004; **25**: 677–86.
24 Biswas SK, Gangi L, Paul S *et al.* A distinct and unique transcriptional program expressed by tumor-associated macrophages (defective NF-kappaB and enhanced IRF-3/STAT1 activation). *Blood* 2006; **107**: 2112–22.
25 Mantovani A, Bottazzi B, Colotta F, Sozzani S, Ruco L. The origin and function of tumor-associated macrophages. *Immunol Today* 1992; **13**: 265–70.
26 Nesbit M, Schaider H, Miller TH, Herlyn M. Low-level monocyte chemoattractant protein-1 stimulation of monocytes leads to tumor formation in nontumorigenic melanoma cells. *J Immunol* 2001; **166**: 6483–90.
27 Barba D, Hardin J, Sadelain M, Gage FH. Development of anti-tumor immunity following thymidine kinase-mediated killing of experimental brain tumors. *Proc Natl Acad Sci USA* 1994; **91**: 4348–52.
28 Vile RG, Castleden S, Marshall J, Camplejohn R, Upton C, Chong H. Generation of an anti-tumour immune response in a non-immunogenic tumour: HSVtk killing in vivo stimulates a mononuclear cell infiltrate and a Th1-like profile of intratumoural cytokine expression. *Int J Cancer* 1997; **71**: 267–74.
29 Ramesh R, Marrogi AJ, Munshi A, Abboud CN, Freeman SM. *In vivo* analysis of the 'bystander effect': a cytokine cascade. *Exp Hematol* 1996; **24**: 829–38.

doi: 10.1111/j.1349-7006.2008.00951.x